# Quantitative Assessment of the Multiplicity of Carbon−Halogen Bonds: Carbenium and Halonium Ions with F, Cl, Br, and I

Robert Kalescky, Wenli Zou, Elfi Kraka,* and Dieter Cremer

Computational and Theoretical Chemistry Group (CATCO), Department of Chemistry, Southern Methodist University, 3215 Daniel Avenue, Dallas, Texas 75275-0314, United States

S *Supporting Information*

ABSTRACT: CX (X = F, Cl, Br, I) and CE bonding (E = O, S, Se, Te) was investigated for a test set of 168 molecules using the local CX and CE stretching force constants k^a calculated at the M06-2X/cc-pVTZ level of theory. The stretching force constants were used to derive a relative bond strength order (RBSO) parameter n. As alternative bond strength descriptors, bond dissociation energies (BDE) were calculated at the G3 level or at the two-component NESC (normalized elimination of the small component)/CCSD(T) level of theory for molecules with X = Br, I or E = Se, Te. RBSO values reveal that both bond lengths and BDE values are less useful when a quantification of the bond strength is needed. CX double bonds can be realized for Br- or I-substituted carbenium ions where as suitable reference the double bond of the corresponding formaldehyde homologue is used. A triple bond cannot be realized in this way as the diatomic CX$^+$ ions with a limited π-donor capacity for X are just double-bonded. The stability of halonium ions increases with the atomic number of X, which is reflected by a strengthening of the fractional (electron-deficient) CX bonds. An additional stability increase of up to 25 kcal/mol (X = I) is obtained when the X$^+$ ion can form a bridged halonium ion with ethene such that a more efficient 2-electron−3-center bonding situation is created.
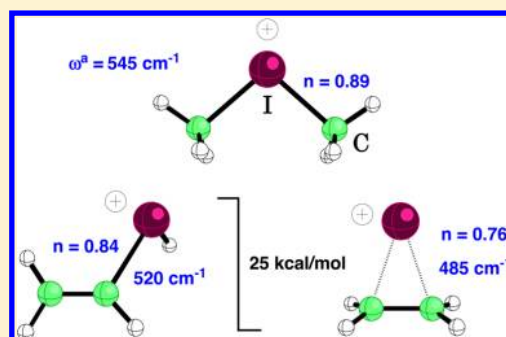
1. INTRODUCTION

In chemistry, the carbon−halogen (CX) bond is considered as a typical example of a polar single bond, which for a given halogen does not show much variation.[1,2] According to measured bond dissociation energies (BDEs), CX bonding becomes weaker from X = F to X = I. For example, the BDE values of CH_3—X decrease in the following order: 110.0 (X = F), 83.7 (Cl), 70.3 (Br), 57.1 kcal/mol (I),[3] which is due to the decrease in bond polarity (decrease in electronegativity: $\chi(C)$ = 2.55, $\chi(F)$ = 3.98, $\chi(Cl)$ = 3.16, $\chi(Br)$ = 2.96, $\chi(I)$ = 2.66)[4] and a reduced overlap between the C sp^m orbitals and the halogen $n\sigma$ orbital (n = 2 (F), 3 (Cl), 4 (Br), and 5 (I)). Because halogen has a valence of 1, chemistry traditionally considers any bond multiplicity higher than 1 for halogen−carbon bonds to be less likely.[5] However, there have been a number of studies in the literature that suggest some variation in the CX single-bond character.[6−11]

In this work, we investigate under which circumstances halogen atoms can undergo double or even triple bonding with carbon. For example, this should become possible if the halogen is bonded to a positively charged C atom as in carbenium ions. Then, the halogen can donate a π-type electron lone pair to the C$^+$ and establish a dative bond leading to a formal double bond with a divalent halogen as sketched in Figure 1. Clearly, the ability of donating an electron pair is relatively small for a F atom but will increase within the halogen group. However, it is not possible to predict whether a CBr or CI double bond does exist because with decreasing overlap between a 2pπ(C) and a 4pπ(Br) or 5pπ(I) orbital the realization of a double bond becomes difficult. Therefore, the existence of
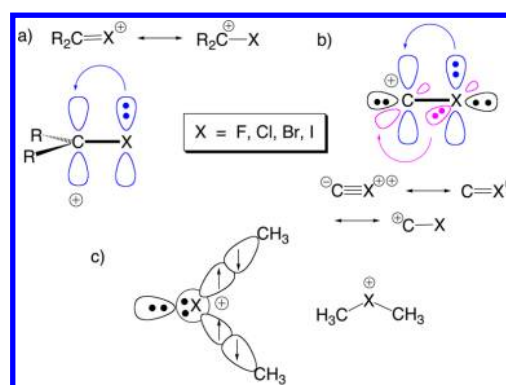

Figure 1. Monovalent halogen X may establish (a) a double or even (b) a triple bond formally via π-donation from an X lone pair orbital. (c) Divalent X$^+$ may be found in halonium ions. For the definition of monovalent or divalent X, see text.

a $^+$C≡X double bond or even a triple bond as in the diatomic $^+$C≡X[12] is more than questionable. Knowledge of the CX bonding mechanism is desirable in many areas of chemistry ranging from synthesis,[2] thermochemistry,[8] spectroscopy,[9,13,14] reaction mechanism, and reaction dynamics[11,15−17] to fields such as astrochemistry.[18]

Divalent halogen is discussed in the literature mostly in connection with halonium ions. These were first proposed by Roberts and Kimball[19] to explain the stereospecificity of the bromine addition to alkenes. Olah and co-workers[20,21] generated bridged halonium ions in superacid solutions and characterized them by spectroscopic methods. Many experimental and computational studies have been published, which provide a good account of their properties.[20−28] Dialkylhalonium ions with X = Cl, Br, I are useful alkylation agents in synthesis[29−34] and they have also been discussed as key intermediates in the catalyzed formation of alkenes from halomethanes.[35] Halonium ions play an important role in electrophilic reactions involving CX bonds. Olah's work starting in the 70s gives ample evidence for this aspect of halonium ion chemistry,[20,21] but even today halonium chemistry attracts the interests of chemists as a special example of electron-deficient bonding.[36−38] Recently, the first evidence for a symmetrical fluoronium ion in solution has been published.[39] Therefore, a comprehensive study of carbon−halogen bonding has to include the bonding in halonium ions.

Chemists determine the single or multiple character of a bond via the electron configuration of an atom and the atomic valences. More details about bonding are obtained from molecular orbitals (MOs) and orbital models such as the perturbational MO (PMO) theory. In this way, a qualitative account of bonding is achieved, which of course cannot provide a quantitative account of the bond strength. From an energetic point of view, it is of limited use to know that a carbon−halogen bond is formally a double bond if its strength does not differ significantly from that of the corresponding single bond. An important prerequisite for a more quantitative understanding of the structure, stability, and reactivity of a molecule is the knowledge of the strength of its bonds. This is the most difficult information to obtain as a direct energy quantity such as the BDE can provide only a qualitative insight as has been shown in several investigations.[40,41]

A reliable probe for measuring the strength of a bond is its stretching force constant.[41] It refers to an infinitesimal change of the bond length; i.e., it does not lead to any electronic structure changes and, therefore, is not flawed by changes in the bond situation. There are numerous attempts to derive bond strength information from vibrational force constants or indirectly from vibrational frequencies, which are less suitable as they depend on atomic masses[42−51] (additional references are summarized in ref 52). The major obstacle in this connection is the fact that the normal vibrational modes of a molecule couple with each other and are delocalized rather than localized, for example, within the diatomic unit of a bond. Accordingly, the normal mode stretching frequencies and force constants do not correctly describe the strength of an individual bond of a molecule as they contain contributions from other stretching, bending, or torsional modes. Konkoli and Cremer solved this problem by deriving a mass-decoupled form of the basic vibrational equations so that local vibrational modes could be determined, which are no longer flawed by any mode−mode coupling.[53]

The Konkoli−Cremer local modes and their properties are independent of all other internal coordinates used to describe the geometry of a molecule, which is not the case for the normal modes. Each local vibrational mode is associated with just one internal coordinate, the changes of which drive the local mode (*leading parameter principle*[53]). The local mode frequencies and force constants can be directly calculated or determined from a complete set of measured vibrational frequencies as first shown by Cremer and co-workers.[54] Experimentally based local mode frequencies (force constants) differ from calculated harmonic local mode frequencies by anharmonicity effects.[55,56] Each normal vibrational mode can be decomposed into local vibrational mode contributions.[52,57] The Konkoli−Cremer modes are the local counterparts of the normal modes, and therefore, their frequencies can be directly related to the normal vibrational frequencies via an adiabatic connection scheme.[58,59]

Local mode force constants are perfectly suited to describe the strength of CX bonds in a quantitative way. In this work, we will determine CX stretching force constants and utilize them to derive a quantitative bond strength measure in the form of a *relative bond strength order (RBSO)* for 96 halogen containing molecules shown in Figure 2. To set CX multiple bonds into the right perspective, we compare these bonds with chalcogen bonds CE (E = O, S, Se, Te) of the 72 E-containing molecules also shown in Figure 2, which are isoelectronic with the carbenium ions investigated in this work.

Utilizing the local stretching force constants and their associated RBSO values of the CX and CE bonds, we will investigate the follwing questions: (1) Are BDE or bond length *r* quantitative or just qualitative bond strength descriptors? Is there any way to predict their reliability or failure? (2) Which halogen stabilizes a carbenium ion best? (3) Is there a possibility of realizing a true CX double or even a CX triple bond? (4) How does CX bonding differ for a variation of X? (5) What are the similarities and differences between CE and CX bonding? Can triple bonds be realized in the case of the diatomic CE molecule? (6) What is the nature of the halonium bond and how can halonium ions be stabilized? (7) What is the best way of determining a bond strength descriptor?

The results of this work are presented in the following way. In section 2, the methodology leading to local stretching force constants are summarized and a suitable bond strength descriptor is derived. In section 3, the focus is on the identification of CX multiple bonds, their comparison with the corresponding CE bonds, and the discussion of fractional CX bonds in halonium ions. Finally, in the last section the conclusions of this work are summarized.

2. COMPUTATIONAL METHODS

Local vibrational modes $\mathbf{a}_n$ (associated with internal coordinates q_n) are derived from normal vibrational modes $\mathbf{d}_\mu$ using the method of Konkoli and Cremer.[53,57] These authors determined the local vibrational modes by solving the mass-decoupled Euler−Lagrange equations. Zou and co-workers[58,59] proved that modes $\mathbf{a}_n$ are the only localized counterparts of the delocalized normal vibrational modes. These authors derived a one to one relationship between modes $\mathbf{a}_n$ and $\mathbf{d}_\mu$ in the form of an adiabatic connection scheme. Both local and (delocalized) normal modes are defined by the Wilson equation of vibrational spectroscopy:[60]

$$\mathbf{F}^q\mathbf{D} = \mathbf{G}^{-1}\mathbf{D}\mathbf{\Lambda} \tag{1}$$

where $\mathbf{F}^q$ is the force constant matrix in internal coordinates, $\mathbf{G}$ is Wilson's kinetic energy matrix, $\mathbf{D}$ collects the normal mode vectors in internal coordinates, and $\mathbf{\Lambda}$ is a diagonal matrix with $3N - L = N_{vib}$ vibrational eigenvalues $\lambda_\mu = 4\pi^2c^2\omega_\mu^2$ (ω_μ, frequency of normal mode μ; c, speed of light; N, number of atoms in the molecule; L, number of translational and rotational degrees of freedom). Diagonalization of the force
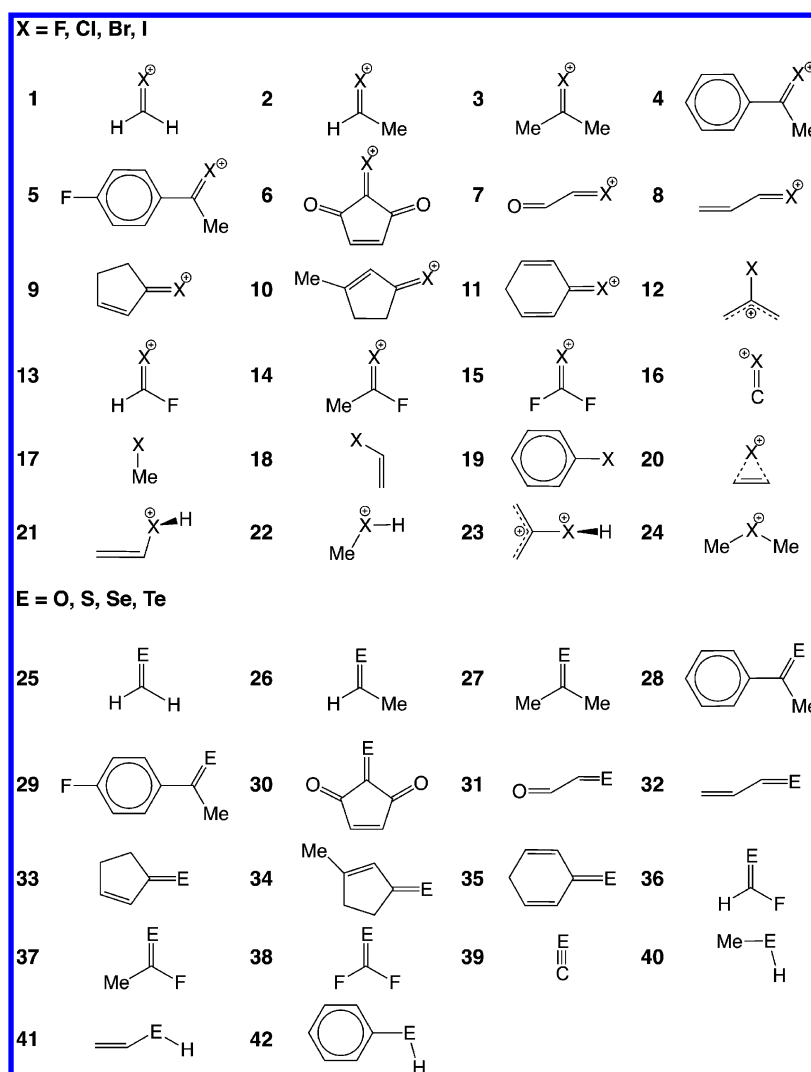
Figure 2. Halogen (X) and chalcogen (E) containing molecules: **1–24** and **25–42**; X = F, Cl, Br, I and E = O, S, Se, Te.

constant matrix yields matrix $\mathbf{K} = \mathbf{D}^\dagger \mathbf{F}^q \mathbf{D}$ that contains the force constants k_μ associated with frequency ω_μ of a given mode μ on its diagonal.

Once the Wilson equation has been solved, the local mode vectors $\mathbf{a}_n$ are determined using the diagonal matrix $\mathbf{K}$ and the mode vectors $\mathbf{d}_\mu$ of the normal modes:[53,58]

$$\mathbf{a}_n = \frac{\mathbf{K}^{-1}\mathbf{d}_n^\dagger}{\mathbf{d}_n \mathbf{K}^{-1}\mathbf{d}_n^\dagger} \tag{2}$$

where $\mathbf{d}_n$ is now a row vector of matrix $\mathbf{D}$ associated with internal coordinate q_n. The local mode force constant k_n^a is given by eq 3

$$k_n^a = \mathbf{a}_n^\dagger \mathbf{K} \mathbf{a}_n \tag{3}$$

and the local mode frequency ω_n^a can be obtained from

$$(\omega_n^a)^2 = \frac{G_{nn} k_n^a}{4\pi^2 c^2} \tag{4}$$

where the **G**-matrix element G_{nn} corresponds to the reciprocal of the local mode mass.[53] In these equations, the superscript a refers to the adiabatic nature of the local vibrational modes: With a finite displacement of the nuclei involved in a local mode, the positions of the remaining atoms of the molecule, not being involved in the local vibration, are adiabatically relaxed, which leads to a decoupling from other modes in the molecule.

Before discussing the use of local stretching force constants as bond strength descriptors it is useful to contrast the term *local mode* as it is employed in this work with the use of this term in the current literature. (i) Henry and co-workers[46,61−64] have developed local mode (an)harmonic oscillator models to quantum mechanically calculate the overtones of XH stretching modes. The higher overtone modes (n = 5 or 6) for isolated XH groups are largely decoupled, which justifies speaking of local modes. The local modes of the oscillator models and their frequencies are true eigenfunctions and eigenvalues of a quantum mechanical Hamiltonian acting on the vibrational wave function. (ii) Reiher and co-workers[65−67] calculate unitarily transformed normal modes associated with a given band in the vibrational spectrum of a polymer where the criteria for the transformation are inspired by those applied for the localization of molecular orbitals. The authors speak in this case of local vibrational modes because the modes are localized in just a few units of a polymer. Nevertheless, Reiher's local modes are still delocalized within the polymer units. (iii) In solid state physics, the term local mode(s) refers to the vibrational mode(s) of an impurity in a solid material.[68,69] (iv) In this

work, the vibrational equation of Wilson[60] is applied to determine normal and local vibrational modes. The basis of the Wilson method, although it is today's quantum chemical standard for calculating the vibrational modes of a molecule, is classical rather than quantum mechanical. This does not devaluate the use of local vibrational modes based on normal modes because the force constants of the former provide a measure of the curvature of the potential energy surface (PES) in the direction of a given internal coordinate q_n and the PES is calculated at the quantum chemical level.

The local stretching force constant k^a is an ideal measure for the bond strength. To simplify the use of this measure, the RBSO is derived from the k^a values. For the purpose of obtaining RBSO values, we followed a multistep strategy: (1) We calculated for all molecules shown in Figure 2 the complete sets of N_{vib} normal vibrational modes utilizing the harmonic approximation. (2) Then, harmonic vibrational frequencies were improved by calculating anharmonic corrections to test the influence of anharmonicity on local mode properties. This was done for all molecules with a second or third period element X or E. (3) Next, local mode frequencies and force constants were derived for both the harmonic and the anharmonically corrected modes. (4) The local mode stretching force constants were used to determine RBSO values, which were employed to describe the strength of a bond in relation to a reference molecule.

As shown in previous work,[10,41,52] the RBSO value n is related to the local stretching force constant k^a by a power relationship

$$n = a(k^a)^b \tag{5}$$

with two parameters a and b. These parameters have to be determined by selecting suitable reference bonds with known bond orders.[10,41,52] Contrary to related relationships such as the Badger[70] or extended Badger rule,[52] which connect stretching force constants and bond lengths for diatomic or polyatomic molecules, respectively, and which have to be determined for each group of molecules separately, eq 5 has to be calibrated only once and then can be used for different bond types.

To describe CX and CE bonds, the C—O single bond of methanol ($n = 1$) and the C=O double bond of formaldehyde ($n = 2$) are chosen as suitable reference bonds. A third requirement is that for $k^a = 0$, the RBSO value n is also zero. Once eq 5 is determined, the RBSO values of all other CX and CE bonds can be calculated utilizing the local stretching force constants k^a. Because the bond strength increases with increasing bond polarity, the C—F bond strength in methyl fluoride will be somewhat larger than that of the C—O bond in methanol ($n(\mathbf{40\text{-}O}) > 1.00$). The C—X (X = Cl, Br, I) bonds will be weaker than the C—F bond, indicating bond weakening with increasing atomic number. Hence, eq 5 will provide a basis to compare the strengths of CX and CE bonds through all periods. The corresponding RSBO values will be denoted as n^{C-O} as the CO single bond in methanol will be used as reference bond ($n^{C-O} = 1.00$) for all other bonds investigated.

Chemists prefer a bond description based on atom valences according to which all CE bonds in H_3C—EH and H_2C=E correspond to true single or double bonds irrespective of the nature of chalcogen E. We have made a concession to this common way of describing chemical bonding by scaling n^{C-O} values such that the CE bond of H_3C—EH has the value n^{C-E} = 1.00 for a given chalcogen E. The corresponding RBSO values do not necessarily lead to values of 2 for H_2C=E but

reflect the decrease in π-bonding for increasing atomic number of E. If a further adjustment is desirable, RBSO values can be scaled to $n^{C=E}$ = 2.00 for H_2C=E. This simplifies the comparison of different CE bonds although one and the same k^a–n relationship is kept, yet with different scaling factors according to different CE reference bonds.

Geometries and harmonic vibrational frequencies of the 168 molecules shown in Figure 2 were calculated using the Minnesota DFT hybrid functional M06-2X[71] and the Dunning correlation consistent basis set cc-pVTZ,[72,73] where for Se, Br, Te, and I effective core potentials were employed.[74] The choice of the M06-2X functional was guided by the results of other authors[75] and the fact that for molecules with measured vibrational frequencies M06-2X lead to harmonic vibrational frequencies, which with the corresponding anharmonicity corrections, are closer to experiment than B3LYP, BLYP, PBE0, or other XC functionals. Similar observations were also made by other authors.[76,77]

In the case of X and E corresponding to a second or third period element, anharmonic corrections of the calculated frequencies were obtained with second order vibrational perturbation theory (VTP2)[78] at the same level of theory. An extension of these calculations for X and E being fourth and fifth period elements turned out to be problematic as in many cases imaginary frequencies were obtained, which vanished when another XC functional was used. This excluded a consistent VTP2 description of all 168 molecules, and therefore, these calculations were limited to O, F, S, and Cl containing molecules.

BDE values were calculated for all molecules. In the case of CO, CF, CS, CCl, CSe, and CBr bonds the Gaussian-3 (G3) method[79] was employed where ZPE (zero-point energy) corrections were excluded from the BDE values to obtain an energetic bond strength parameter that can be directly related to bond lengths and force constants. Because the G3 method is not available for higher periods of the periodic table, for molecules containing CI and CTe bonds, CCSD(T) theory[80] in connection with the all-electron diract-exact normalized elimination of the small component (NESC) method of Zou, Filatov, and Cremer[81−84] was used to account for electron correlation and scalar relativistic effects. Spin−orbit coupling (SOC) corrections were calculated with a two-component (2c) version of the NESC method.[85] 2c-NESC/CCSD(T) calculations were carried out with Dunning's cc-pVTZ basis set for all elements except Se, Br, Te, and I for which the Tatewaki−Koga (TK) relativistic (DKH3)[86] and generally contracted (Gen) basis set DKH3-Gen-TK+NOSeC-V-TZP[87,88] was applied using M06-2X/cc-pVTZ geometries.

The reliability of BDE values calculated with the 2c-NESC/CCSD(T) method was investigated by repeating the calculation of BDE values for CSe and CBr bonds and comparing them with G3 results. In those cases where measured bond dissociation enthalpies at 298 K (BDH(298)) are available,[3] BDH(298) were calculated for reasons of comparison. NBO (natural bond order) charges were calculated using the method of Wenthold and co-workers.[89] The program package COLOGNE2013[90] was used for all local mode and NESC calculations whereas Gaussian 09[91] was employed for the calculation of DFT geometries, frequencies, and BDE values.

3. RESULTS AND DISCUSSION

In Tables 1−4, the CX and CE bond lengths r, BDE values, local stretching force constants k^a, local stretching frequencies ω^a, and RBSO values n^{C-O} (n^{C-E}) are given for the 168

Table 1. Bond Lengths *r* for the CX (X = F, Cl, Br, I) and CE Bonds (E = O, S, Se, Te) in Molecules 1−42 (M06-2X/cc-pVTZ Calculations)[a]

	molecule	sym	O/F [Å]	S/Cl [Å]	Se/Br [Å]	Te/I [Å]
1	$[H_2CX]^+$	C_{2v}	1.226	1.588	1.741	1.939
2	$[MeHCX]^+$	C_s	1.248	1.618	1.774	1.976
3	$[Me_2CX]^+$	C_2	1.267	1.645	1.805	2.013
4	$[PhMeCX]^+$	C_s	1.295	1.684	1.838	2.049
5		C_s	1.297	1.688	1.851	2.052
6		C_{2v}	1.230	1.587	1.741	1.939
7	$[O{=}CHCHX]^+$	C_1	1.284	1.599	1.753	1.952
8	$[H_2C{=}CHCHX]^+$	C_s	1.264	1.637	1.793	1.996
9		C_s	1.275	1.657	1.815	2.023
10		C_s	1.280	1.664	1.823	2.031
11		C_{2v}	1.291	1.678	1.837	2.045
12		C_{2v}	1.312	1.707	1.870	2.084
13	$[HCFX]^+$	C_s	1.227	1.604	1.763	1.974
14	$[MeCFX]^+$	C_s	1.245	1.628	1.792	2.006
15	$[CF_2X]^+$	D_{3h}	1.229	1.614	1.780	2.004
16	$[CX]^+$	$C_{\infty v}$	1.151	1.534	1.693	1.905
17	H_3CX	C_{3v}	1.377	1.783	1.940	2.137
18	$H_2C{=}CHX$	C_s	1.339	1.733	1.891	2.090
19	PhX	C_{2v}	1.342	1.739	1.898	2.099
20		C_{2v}	1.523	1.854	2.013	2.222
21	$[H_2C{=}CH(XH)]^+$	C_s	1.620	1.831	1.966	2.128
22	$[H_3CXH]^+$	C_s	1.588	1.857	1.993	2.159
23		C_s	1.527	1.819	1.964	2.147
24	$[H_3CXCH_3]^+$	C_{2v}	1.506	1.821	1.965	2.141
25	$H_2C{=}E$	C_{2v}	1.195	1.601	1.741	1.941
26	$MeHC{=}E$	C_s	1.199	1.609	1.752	1.956
27	$Me_2C{=}E$	C_2	1.204	1.619	1.765	1.974
28	$PhMeC{=}E$	C_s	1.208	1.629	1.778	1.991
29		C_s	1.208	1.629	1.785	1.993
30		C_{2v}	1.189	1.594	1.736	1.940
31	$O{=}CHCH{=}E$	C_1	1.196	1.604	1.745	1.948
32	$H_2C{=}CHCH{=}E$	C_s	1.202	1.617	1.761	1.967
33		C_s	1.203	1.624	1.772	1.984
34		C_s	1.204	1.627	1.775	1.988
35		C_{2v}	1.213	1.637	1.786	1.997
36	$FC{=}E$	C_s	1.173	1.590	1.736	1.950
37	$MeFC{=}E$	C_s	1.178	1.602	1.751	1.970
38	$F_2C{=}E$	C_{2v}	1.167	1.592	1.745	1.972
39	CE	$C_{\infty v}$	1.122	1.528	1.668	1.882
40	H_3CEH	C_s	1.413	1.816	1.957	2.147
41	$H_2C{=}CH(EH)$	C_s	1.361	1.763	1.908	2.105
42	$PhEH$	C_s	1.361	1.770	1.915	2.126

[a]For a numbering of molecules, see Figure 2.

molecules shown in Figure 2. In Table 5, calculated BDH(298) values of CX and CE bonds are compared with the available experimental data. Additional results are summarized in the Supporting Information.

4. RELATIONSHIP BETWEEN FORCE CONSTANTS AND BOND LENGTHS

In 1934, Badger[70] showed that stretching force constant and bond length *r* of diatomic molecules are related by a power equation. The so-called *Badger rule* expects that bonds between atoms of the same period(s) follow similar *k*−*r* relationships, which by defining an effective bond length merge into a single

relationship.[70] The extension of these relationships to polyatomic molecules turned out to be problematic because spectroscopically or quantum chemically derived stretching force constants contain mode−mode coupling and depend on the internal coordinates used for the description of the molecule in question.[52] A solution of the problem was found by Kraka and Cremer who showed that an extended Badger relationship is valid for polyatomic molecules provided local stretching force constants are available.[52,92]

In Figure 3, the local mode force constants k^a are compared with bond lengths *r* where Figure 3a gives the situation for CBr and CSe bonds and Figure 3b for CI and CTe bonds (for the corresponding diagrams of the lower periods, see the Supporting Information). The stretching force constant decreases in all cases with increasing bond length. Obviously, there is a power relationship between the two bond properties, which for CE and CX bonds are similar. However, it is also obvious that the scattering of data points increases from CE (R^2 = 0.990 for E = Se) to CX (R^2 = 0.962 for X = Br) for which the halonium bonds are responsible. Increased scattering can be observed for the higher periods (R^2 = 0.986 and 0.924 for Te and I, respectively), which reveals the deficiencies of using bond lengths as bond strength descriptors. Within a model, the bond length can be viewed as the sum of the covalent radii of the bonded atoms. The covalent radius changes with the polarity of a bond, which in turn depends on the electronegativity difference between the atoms bonded, the substituents attached to them, the overall molecular charge, and the resulting effective charges of the atoms in question. For example, strongly electronegative substituents can decrease the covalent radius of an atom. The bond length becomes shorter, which in turn can lead to increased substituent−substituent repulsion, thus weakening the bond. This implies that shorter bonds can be weaker rather than stronger bonds as has been described in the literature.[52]

Investigations as the one summarized in Figure 3 confirm the extended Badger rule;[52,92] however, they also reveal that there is just a qualitative rather than a quantitative relationship between k^a and *r* being valid for the comparison of similar bond types. By an increased variation of the bond type in question, for example, by the inclusion of CX halonium bonds with a relatively large change in the atomic charges and a subsequent variation in the covalent radii of the bonded atoms, the reliability of the bond length as a qualitative bond strength descriptor decreases significantly. Also, the hard-sphere model of the bonded atom, which is the basis of the Badger rule, becomes less useful for the elements of the higher periods, which can more easily be polarized or transfer charge to a bonding partner.

Relationship between Force Constants and BDE Values. In the case of the BDE values (Table 2), their accuracy matters. This is guaranteed to a certain extent by the G3 approach,[79] which includes complete basis, infinite order correlation, and relativistic effects. A comparison of measured and calculated BDH(298) values (Table 5) reveals that, apart from the CX^+ ions, theory differs from experiment by just 1.2 kcal/mol on the average.

The Dirac-exact 2c-NESC/CCSD(T) calculations were carried out with a finite basis set of triple-ζ quality. However, they provide a reliable account of scalar relativistic, spin−orbit coupling, and infinite order correlation effects.[81−83,85] BDE values obtained with G3 and 2c-NESC/CCSD(T) are in reasonable agreement (standard deviation σ = 1.70 kcal/mol;

Table 2. Bond Dissociation Energies (BDE, kcal/mol) for the CX (X = F, Cl, Br, I) and CE Bonds (E = O, S, Se, Te) in Molecules 1−42 (G3 and 2c-NESC/CCSD(T) Calculations)[a]

	molecule	sym	O/F G3	S/Cl 3	Se/Br G3	Se/Br 2c-NESC/CCSD(T)	Te/I 2c-NESC/CCSD(T)
1	$[H_2CX]^+$	C_{2v}	155.27	136.85	125.45	122.77	117.66
2	$[MeHCX]^+$	C_s	139.28	113.27	100.13	101.56	93.24
3	$[Me_2CX]^+$	C_2	136.18	105.04	90.78	88.17	77.81
4	$[PhMeCX]^+$	C_s	132.16	99.12	84.54	80.88	69.12
5		C_s	130.33	97.43	82.90	79.87	68.08
6		C_{2v}	148.28	131.51	120.76	117.14	113.04
7	$[O=CHCHX]^+$	C_1	109.64	87.12	76.00	72.43	66.78
8	$[H_2C=CHCHX]^+$	C_s	138.73	111.98	98.78	96.05	87.28
9		C_s	137.29	108.20	94.31	91.34	81.06
10		C_s	136.25	106.68	92.69	89.70	79.09
11		C_{2v}	133.03	102.58	88.61	85.53	74.76
12		C_{2v}	124.99	95.78	82.38	100.49	90.44
13	$[HCFX]^+$	C_s	146.62	120.32	107.39	103.91	96.04
14	$[MeCFX]^+$	C_s	141.03	109.65	95.74	92.19	81.84
15	$[CF_2X]^+$	D_{3h}	141.46	117.29	105.38	101.23	94.71
16	$[CX]^+$	$C_{\infty v}$	181.52	153.45	140.28	136.17	128.33
17	H_3CX	C_{3v}	114.45	86.25	73.31	70.65	58.35
18	$H_2C=CHX$	C_s	127.56	97.17	83.03	80.23	67.10
19	PhX	C_{2v}	132.25	102.18	88.20	84.01	71.15
20		C_{2v}	85.03	82.39	76.41	74.14	72.11
21	$[H_2C=CH(XH)]^+$	C_s	16.40	32.05	39.15	37.77	48.02
22	$[H_3CXH]^+$	C_s	32.26	50.57	56.15	56.59	66.99
23		C_s	33.66	63.11	73.34	74.46	92.62
24	$[H_3CXCH_3]^+$	C_{2v}	50.64	68.56	72.51	72.81	81.10
25	$H_2C=E$	C_{2v}	182.95	134.26	113.87	109.82	88.74
26	$MeHC=E$	C_s	187.38	136.46	115.69	111.44	89.56
27	$Me_2C=E$	C_2	189.87	137.44	116.49	112.15	89.89
28	$PhMeC=E$	C_s	184.02	132.32	111.81	105.10	86.12
29		C_s	184.72	133.00	112.50	108.05	86.41
30		C_{2v}	74.92	131.37	112.45	107.93	89.57
31	$O=CHCH=E$	C_1	176.45	129.50	109.86	105.62	85.57
32	$H_2C=CHCH=E$	C_s	177.85	129.15	109.35	105.54	85.01
33		C_s	187.01	137.03	116.98	112.69	91.80
34		C_s	188.64	138.75	118.75	114.40	93.54
35		C_{2v}	178.39	130.70	111.44	07.35	87.09
36	$HFC=E$	C_s	204.79	143.28	120.44	115.93	91.75
37	$MeFC=E$	C_s	207.33	144.96	122.26	117.57	93.52
38	$F_2C=E$	C_{2v}	217.94	154.70	131.75	127.11	103.31
39	CE	$C_{\infty v}$	259.55	172.42	144.40	136.75	104.45
40	H_3CEH	C_s	97.04	77.67	69.52	67.42	57.45
41	$H_2C=CH(EH)$	C_s	118.14	94.17	84.47	77.31	66.26
42	$PhEH$	C_s	118.36	93.63	84.02	80.55	69.69

[a]For a numbering of molecules, see Figure 1. BDE values do not contain ZPE corrections.

Table 2 and Figure 4). Accordingly, the BDE values for CTe and CI bonds calculated at the 2c-NESC/CCSD(T) level can also be considered as being reliable.

Because the RBSO values are related to the local stretching force constants k^a by a power relationship as are k^a and r, RBSO and r are linearly related by an inverse relationship. There should also be linear relationships between RBSO and BDE values, which are shown in Figure 5. The BDE increases with increasing RBSO where, however, the strong scattering of data points excludes the determination of a linear relationship. Scattering increases with increasing atomic number, which can be easily understood when the nature of the bond dissociation reaction is considered. The energy of this reaction depends on the strength of the bond being broken and the stability of the two fragments being formed. Upon dissociation, the dissociation

fragments increase their stability by geometry relaxation, rehybridization, and electron density reorganization of the original molecule.

These relaxation effects are different for different organic fragments, different atoms X or E, and different charge and bonding situations. An additional uncertainty is brought about by SOC, which is large in case of a fractional occupation of p-, d-, or f-type orbitals. Because all molecules investigated are closed-shell molecules, their dissociation leads to an increase of SOC effects provided a fifth or sixth row atom is involved. This decreases the BDE value, suggesting an artificial weakening of the CX or CE bond. Another impact on the calculated BDE value is given in the situation of an avoided crossing between the ground state and an excited state of the dissociating molecule in question. In such a situation, the BDE value is

Table 3. Harmonic Local Mode Force Constants k^a and Frequencies ω^a for the CX (X = F, Cl, Br, I) and CE Bonds (E = O, S, Se, Te) in Molecules 1−42 (M06-2X/cc-pVTZ Calculations)[a]

	molecule	sym	k^a [mdyn/Å]				ω^a [cm^{-1}]			
			O/F	S/Cl	Se/Br	Te/I	O/F	S/Cl	Se/Br	Te/I
1	[H$_2$CX]$^+$	C_{2v}	11.343	6.754	5.480	4.422	1618	1133	945	827
2	[MeHCX]$^+$	C_s	9.748	5.717	4.674	3.767	1500	1042	873	764
3	[Me$_2$CX]$^+$	C_2	8.509	4.853	4.076	3.100	1401	960	815	693
4	[PhMeCX]$^+$	C_s	7.383	4.146	3.495	2.313	1305	888	755	598
5		C_s	7.290	4.104	3.331	2.758	1297	883	737	653
6		C_{2v}	10.874	6.552	5.330	4.326	1584	1116	932	818
7	[O=CHCHX]$^+$	C_1	7.717	6.302	5.103	4.241	1335	1094	912	810
8	[H$_2$C=CHCHX]$^+$	C_s	8.959	5.243	4.365	3.518	1438	998	843	738
9		C_s	8.492	4.854	4.021	3.164	1400	960	810	700
10		C_s	8.274	4.722	3.912	3.076	1382	947	798	690
11		C_{2v}	7.858	4.491	3.737	2.965	1347	924	780	678
12		C_{2v}	7.349	4.225	3.442	2.830	1302	896	749	662
13	[HCFX]$^+$	C_s	10.785	6.095	4.846	3.791	1578	1076	889	766
14	[MeCFX]$^+$	C_s	9.377	5.327	4.302	3.293	1471	1006	837	714
15	[CF$_2$X]$^+$	D_{3h}	10.634	5.790	4.508	3.268	1567	1049	857	711
16	[CX]$^+$	$C_{\infty v}$	14.756	7.768	6.192	4.743	1845	1215	1004	857
17	H$_3$CX	C_{3v}	5.614	3.218	2.764	2.296	1138	782	671	596
18	H$_2$C=CHX	C_s	6.373	3.630	3.031	2.595	1213	830	703	634
19	PhX	C_{2v}	6.395	3.626	3.054	2.614	1215	830	705	636
20		C_{2v}	2.021	1.911	1.792	1.517	683	603	540	485
21	[H$_2$C=CH(XH)]$^+$	C_s	0.983	1.703	1.690	1.744	476	569	525	520
22	[H$_3$CXH]$^+$	C_s	1.628	1.836	1.746	1.706	613	591	533	514
23		C_s	1.963	2.312	2.196	2.072	673	663	598	566
24	[H$_3$CXCH$_3$]$^+$	C_{2v}	2.513	2.278	2.088	1.919	762	658	583	545
25	H$_2$C=E	C_{2v}	14.204	7.268	5.886	4.628	1875	1189	979	846
26	MeHC=E	C_s	13.789	6.892	5.518	4.343	1848	1158	948	819
27	Me$_2$C=E	C_2	13.338	6.570	5.164	4.028	1817	1131	917	789
28	PhMeC=E	C_s	12.914	6.167	4.813	3.669	1788	1095	885	753
29		C_s	12.886	6.075	4.778	3.628	1786	1087	882	749
30		C_{2v}	14.465	7.293	5.895	4.617	1892	1191	979	845
31	O=CHCH=E	C_1	13.954	7.042	5.724	4.545	1859	1170	965	838
32	H$_2$C=CHCH=E	C_s	13.451	6.657	5.301	4.183	1825	1138	929	804
33		C_s	13.261	6.341	4.978	3.853	1812	1111	900	772
34		C_s	13.152	6.242	4.916	3.765	1804	1102	894	763
35		C_{2v}	12.562	6.014	4.750	3.711	1763	1082	879	757
36	HFC=E	C_s	15.448	7.257	5.746	4.315	1956	1188	967	817
37	MeFC=E	C_s	14.874	6.807	5.312	3.981	1919	1151	930	784
38	F$_2$C=E	C_{2v}	15.873	6.998	5.318	3.758	1982	1167	930	762
39	CE	$C_{\infty v}$	20.911	9.410	7.307	5.501	2275	1353	1090	922
40	H$_3$CEH	C_s	5.194	3.045	0.638	2.258	1134	770	655	591
41	H$_2$C=CH(EH)	C_s	6.175	3.436	2.882	2.505	1236	818	685	622
42	PhEH	C_s	6.185	3.413	2.919	2.467	1237	815	689	617

[a]For a numbering of molecules, see Figure 2.

artificially lowered as in the case of molecule **7-X** (X = Br or I) (Figure 5), because with the increasing atomic number of X or E, the excited state energies decrease and the possibility of an avoided crossing increases, leading to unusually low BDE values.

Hence, one cannot expect that the BDE is, in any quantitative or qualitative sense, a reliable bond strength descriptor, which is confirmed by the results of this work summarized in Figure 5.

Influence of the Anharmonicity on Results. For all molecules containing period 2 or period 3 chalcogen or halogen atoms, anharmonicity corrections were obtained (Supporting Information), which reduces the magnitude of ω^a and k^a. These changes are best assessed by the corresponding changes in the RBSO values. In general, anharmonically corrected stretching

force constants k^a lead to 2−7% smaller RSBO values than the corresponding harmonic k^a values in the cases of the CF and CO bonds. For example, the RBSO value n for **1** is 1.713 (harmonic) and decreases to 1.639 when anharmonically corrected. The differences are somewhat smaller for the CCl and CS bonds. This decrease is a result of the well-known fact that harmonic force constants exaggerate the bond strength, which is more pronounced for stronger than for weaker bonds.

The anharmonic corrections are important when local mode properties are directly compared with those derived from measured vibrational frequencies. However, when trends in calculated RBSO values are analyzed, anharmonic corrections do not change these trends significantly. In view of the fact that anharmonic corrections for molecules with atoms from higher

Table 4. Relative Bond Strength Orders (RBSO) for the CX (X = F, Cl, Br, I) and CE Bonds (E = O, S, Se, Te) in Molecules 1−42 (M06-2X/cc-pVTZ)[a]

	molecule	sym	$n^{C-O}_{CO,CF}$	$n^{C-E}_{CS,CCl}$	$n^{C-O}_{CS,CCl}$	$n^{C-E}_{CSe,CBr}$	$n^{C-O}_{CSe,CBr}$	$n^{C-E}_{CTe,CI}$	$n^{C-O}_{CTe,CI}$
1	$[H_2CX]^+$	C_{2v}	1.713	1.731	1.198	1.655	1.038	1.589	0.895
2	$[MeHCX]^+$	C_s	1.543	1.543	1.068	1.483	0.930	1.423	0.801
3	$[Me_2CX]^+$	C_2	1.405	1.379	0.954	1.350	0.846	1.244	0.701
4	$[PhMeCX]^+$	C_s	1.274	1.237	0.856	1.214	0.761	1.017	0.573
5		C_s	1.263	1.228	0.850	1.174	0.736	1.148	0.647
6		C_{2v}	1.664	1.695	1.174	1.624	1.018	1.565	0.882
7	$[O{=}CHCHX]^+$	C_1	1.314	1.651	1.143	1.576	0.988	1.544	0.870
8	$[H_2C{=}CHCHX]^+$	C_s	1.456	1.454	1.006	1.415	0.887	1.357	0.765
9		C_s	1.403	1.379	0.954	1.337	0.838	1.262	0.711
10		C_s	1.378	1.353	0.936	1.312	0.823	1.237	0.697
11		C_{2v}	1.330	1.307	0.905	1.271	0.797	1.206	0.680
12		C_{2v}	1.270	1.253	0.867	1.201	0.753	1.168	0.658
13	$[HCFX]^+$	C_s	1.654	1.613	1.117	1.520	0.953	1.429	0.805
14	$[MeCFX]^+$	C_s	1.502	1.470	1.018	1.401	0.878	1.297	0.731
15	$[CF_2X]^+$	D_{3h}	1.638	1.557	1.078	1.447	0.907	1.290	0.727
16	$[CX]^+$	$C_{\infty v}$	2.053	1.906	1.320	1.800	1.129	1.668	0.939
17	H_3CX	C_{3v}	1.055	1.039	0.719	1.033	0.647	1.012	0.570
18	$H_2C{=}CHX$	C_s	1.151	1.129	0.781	1.100	0.690	1.101	0.620
19	PhX	C_{2v}	1.154	1.128	0.781	1.106	0.694	1.106	0.623
20		C_{2v}	0.522	0.725	0.502	0.766	0.480	0.760	0.428
21	$[H_2C{=}CH(XH)]^+$	C_s	0.318	0.670	0.464	0.736	0.461	0.837	0.471
22	$[H_3CXH]^+$	C_s	0.450	0.706	0.488	0.753	0.472	0.824	0.464
23		C_s	0.511	0.827	0.573	0.881	0.553	0.942	0.531
24	$[H_3CXCH_3]^+$	C_{2v}	0.606	0.819	0.567	0.851	0.534	0.894	0.504
25	$H_2C{=}E$	C_{2v}	2	1.821	1.260	1.738	1.090	1.640	0.924
26	$MeHC{=}E$	C_s	1.960	1.756	1.215	1.663	1.043	1.569	0.884
27	$Me_2C{=}E$	C_2	1.915	1.699	1.176	1.589	0.996	1.490	0.839
28	$PhMeC{=}E$	C_s	1.873	1.626	1.126	1.513	0.949	1.397	0.787
29		C_s	0.870	1.609	1.114	1.506	0.944	1.386	0.781
30		C_{2v}	2.025	1.825	1.263	1.740	1.091	1.637	0.922
31	$O{=}CHCH{=}E$	C_1	1.976	1.782	1.233	1.705	1.069	1.619	0.912
32	$H_2C{=}CHCH{=}E$	C_s	1.926	1.714	1.186	617	1.014	1.529	0.861
33		C_s	1.908	1.658	1.147	1.549	0.971	1.445	0.814
34		C_s	1.897	1.640	1.135	1.536	0.963	1.422	0.801
35		C_{2v}	1.838	1.598	1.106	1.500	0.940	1.408	0.793
36	$HFC{=}E$	C_s	2.119	1.819	1.259	1.710	1.072	1.562	0.880
37	$MeFC{=}E$	C_s	2.065	1.741	1.205	1.620	1.016	1.478	0.833
38	$F_2C{=}E$	C_{2v}	2.159	1.774	1.228	1.621	1.016	1.420	0.800
39	CE	$C_{\infty v}$	2.611	2.176	1.506	2.018	1.265	1.847	1.040
40	H_3CEH	C_s	1	1	0.692	1	0.627	1	0.563
41	$H_2C{=}CH(EH)$	C_s	1.127	1.087	0.752	1.063	0.666	1.074	0.605
42	$PhEH$	C_s	1.128	1.082	0.749	1.072	0.672	1.063	0.599

[a]For a numbering of molecules, see Figure 2. RBSO values n^{C-O} use the CO bonds in methanol and formaldehyde as reference bonds whereas n^{C-E} values are scaled n^{C-O} values to obtain an RBSO value for the C—E bond in H_3C—EH of 1.00.

periods lead to numerical problems (e.g., artificial imaginary frequencies), we exclusively use in this work harmonic local stretching force constants as quantitative bond strength descriptors.

Do Carbon and Halogen Form Double Bonds? The answer to this question depends on the bonding model being used. The chemist considers the CE bond in **40** as a typical single bond and that in **25** as a typical double bond. However, the strength of the C=E bond decreases according to the calculated RBSO values n^{C-E} of Table 4 to 91 (E = S), 87 (E = Se), and 82% (E = Te) of that in formaldehyde (standard double bond with n = 2.00) because of the well-known decrease in the π-bond strength with increasing atomic number,[93,94] which is due to the decrease in overlap between $2p\pi$ and $np\pi$

orbitals (principal quantum number n = 3 (S), 4 (Se), 5 (Te)) for increasing bond length r and the decrease in bond polarity with decreasing electronegativity difference. According to the RBSO values n^{C-E} of the typical "double bonds" C=E obtained for the formaldehyde analogues **25** (n = 2.00, 1.82, 1.74, 1.64), the π-bond strength decreases to 82 (E = S), 74 (E = Se), and 64% (E = Te) (Figure 6).

The RBSO values n^{C-E} of **1** are 1.71, 1.73, 1.66, and 1.59 (Table 4); i.e., they approach the "double bond" character of H_2C=E by 85.6 (X = F), 95.0 (X = Cl), 95.2 (X = Br), and 96.9% (X = I). With the increasing atomic number of X, the CX double bond increasingly resembles the C=E double bond. Clearly, the latter is a result of the increasing polarizability and π-donor strength of atom X. This is best given for H_2C=I$^+$ although the BDE value

Table 5. Comparison of Experimental and Calculated Bond Dissociation Enthalpies (BDHs) at 298 K[a]

	molecule	BDH(298) exp [kcal mol^{-1}]	BDH(298) G3 [kcal mol^{-1}]	ΔBDH [kcal mol^{-1}]
16-F	$[CF]^+$	172	179.9	−7.9
17-F	H_3CF	110	109.7	0.3
1-F	$[H_2CCl]^+$	131.2	133.0	−1.8
16-Cl	$[CCl]^+$	148.8	152.7	−3.9
17-Cl	H_3CCl	83.7	84.9	−1.2
1-Br	$[H_2CBr]^+$	123.7	122.1	1.6
16-Br	$[CBr]^+$	107.9	39.8	−31.9
17-Br	H_3CBr	70.3	69.8	0.5
25-O	CH_2O	180.6	178.4	2.2
39-O	CO	257.3	257.3	0.0
40-O	H_3COH	92	90.5	0.5
25-S	H_2CS	131.2	131.0	0.2
39-S	CS	170.5	171.5	1.0
40-S	H_3CSH	74.7	72.8	1.9
39-Se	CSe	141.1	143.8	−2.7

[a]Experimental values have been taken from Luo's compilation of BDHs[3] or, in the case of diatomic molecules, from Huber and Herzberg[95] whereas the theoretical values are based on G3 calculations.[79]

Figure 4. BDE values determined with the 2c-NESC/CCSD(T) compared with G3-based BDE values in the case of CBr (filled circles) or CSe bonds (open circles). For the numbering of molecules, see Figure 2.

Figure 3. Local stretching force constants k^a compared with bond lengths r for molecules with (a) CBr (filled circles) or CSe bonds (open circles). Correlations are given for CBr (solid line) and CSe bonds (dashed line): $k^a = 7568^{-4.163r}$ and $k^a = 3772^{-3.737r}$, respectively. (b) Similar correlations are given for molecules with CI (filled circles, solid line) or CTe bonds (open circles, dashed line): $k^a = 6861^{-3.737r}$ and $k^a = 3353^{-3.410r}$, respectively (M06-2X/cc-pVTZ calculations).

Figure 5. BDE values are compared with RBSO values n^{C-E} for the molecules with (a) CBr (filled circles) or CSe bonds (open circles) and (b) CI (filled circles) or CTe bonds (open circles). BDE values are based on either G3 or 2c-NESC/CCSD(T) calculations whereas the RBSO values are based on local stretching force constants calculated at the M06-2X/cc-pVTZ level of theory.

of this carbenium ion is just 117.7 kcal/mol and by this much smaller than that for the F analogue (155.3 kcal/mol, Table 2), which of course reflects the large difference in both the σ- and the π-bond strengths.
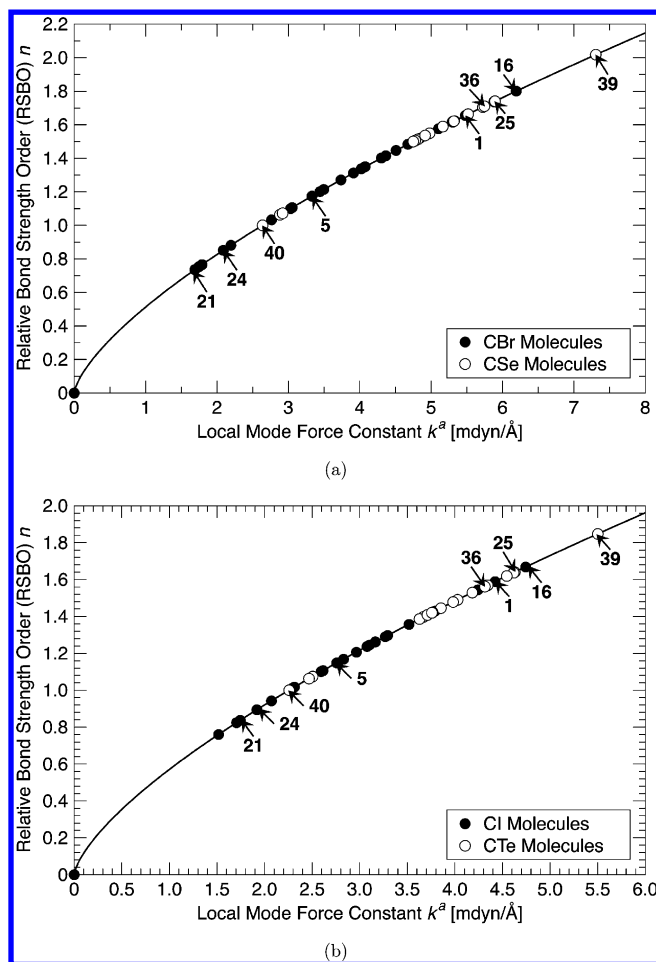
(a)

(b)

Figure 6. RBSOs n^{C-E} as a function of the local mode force constants k^a derived from normal-mode frequencies. (a) Molecules with CBr (filled circles) and CSe bonds (open circles). RBSO values are given by $n^{C-E} = 0.523(k^a)^{0.677}$. (b) Molecules with CI (filled circles) and CTe bonds (open circles). RBSO values are given by $n^{C-E} = 0.583(k^a)^{0.677}$. For the numbering of molecules, see Figure 2 (M06-2X/cc-pVTZ calculations).

Of course the interpretation of results depends on the reference chosen. If H_3C-X is used as reference for the $C-X$ single bond, RBSO values change to $1.713/1.055 = 1.62$, 1.67, 1.60, and 1.57, suggesting a somewhat weaker π-character of the CX bond in **1**.

Despite the strength of the CF bond, the F substituent is too electronegative to provide more than 62% of a π-bond (relative to the $C-F$ single bond in **17**). None of the RBSO values of the F-substituted carbenium ions is close to the double bond value of formaldehyde. The bromo- and iodo-substituted carbenium ions come closer to the "double bonds" in seleno- or telluroformaldehyde. Insofar, the question introducing this subsection can be positively answered.

However, this is the viewpoint of a bonding model based on valences and orbital interactions. From a single-reference point of view, which relates all stretching force constants k^a to RBSO values n^{C-O} by a single equation without any scaling for higher homologues (Figure 7), there is a rapid decrease in the bond strength with increasing atomic number of E or X such that the single bond in **40** with E = Te is just 56% of the strength of the CO bond in methanol according to an RBSO decrease from $n^{C-O} = 1.00$ (E = O) to 0.69 (E = S), 0.63 (E = Se), and 0.56

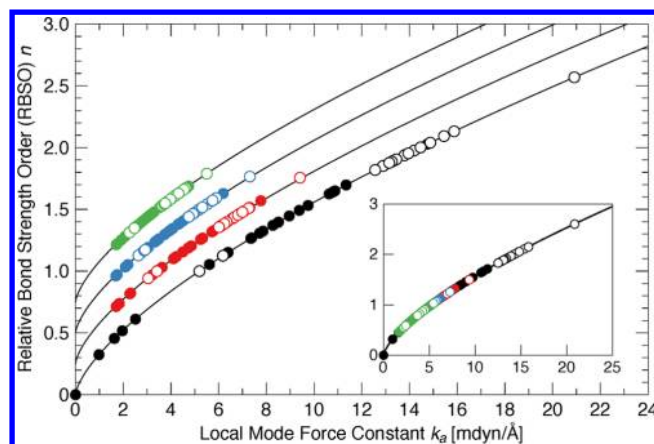**Figure 7.** RBSOs n^{C-O} are given by one function of local stretching force constants k^a for all molecules studied. For better recognition of individual data points, the CCl/CS RBSO values are shifted by 0.25 (red circles), the CBr/CSe RBSO values by 0.5 (blue circles), and the CI/CTe RBSO values by 0.75 units (green circles). The inset clarifies that all n^{C-O} values are on one line given by the equation $n^{C-O} = 0.328(k^a)^{0.677}$ (M06-2X/cc-pVTZ calculations).

(E = Te; Table 4). For the $H_2C=E$ molecules, the corresponding n values are 2.00, 1.26, 1.09, and 0.92, whereas for the $H_2C = X^+$ ions $n^{C-O} = 1.71$, 1.20, 1.04, 0.89 is obtained.

Is a Carbon–Halogen Triple Bond Realized for CX$^+$? It has been speculated that the diatomic cations CF$^+$, CCl$^+$, and CBr$^+$ (**16**) could be the only molecules with a C≡X triple bond because they are isoelectronic with CO, CS, and CSe (Figure 1).[12] The diatomic CO molecule (**39**) is expected to have a triple bond due to three doubly occupied bonding MOs. However, the RSBO value of **39**-O is 2.61, which reflects the fact that a bonding σ-MO and an antibonding σ-MO are doubly occupied where the latter always leads to a larger destabilization than the former to stabilization.

For CS, CSe, and CTe, the RBSO values n^{C-E} are 2.18, 2.02, and 1.85 (scaled to get $n = 1.00$ for the $C-E$ bond in **40**), which relate to bond orders $n^{C=E}$ of 2.39, 2.32, and 2.25 if the corresponding $H_2C=E$ bonds would be true double bonds; i.e., the tendency for multiple bonding in the diatomic CE clearly decreases from E = O to S, Se, or Te, and is comparable to or below that of the double bond in formaldehyde. On the n^{C-O} scale, RBSO values are 1.51, 1.26, and 1.04 relative to the $C-O$ bond in methanol being $n = 1.00$.

For CF$^+$, CCl$^+$, CBr$^+$, and CI$^+$, the n^{C-E} values are 2.05, 1.91, 1.80, and 1.67; i.e., the largest decrease in strength from CE to CX$^+$ is found for CF$^+$ whereas the higher homologues approach the values of diatomic CE. In summary, triple bonding in CX$^+$ is not possible because the electronegativity of X excludes a double π-donation (Figure 1), which would be a prerequisite for a triple bond. The CF$^+$ has a double bond ($n^{C-E} = 2.05$) whereas with increasing atomic number of X the double bond character decreases to 1.67 in the case of CI$^+$. Hence, the diatomic system CX$^+$ is much more sensitive to the decrease in orbital overlap compared to the halogen-substituted carbenium ions.

Because it is difficult to measure the BDE values of the diatomic CX$^+$ ions, calculated BDE values are more reliable in this case. We calculate BDE values of 181.5 (X = F), 153.5 (Cl), 140.3 (Br), and 128.3 kcal/mol (I), which correspond to BDH(298) values of 179.9, 152.7, 139.8, and 128.1 kcal/mol, respectively (Tables 2 and 5). The experimental values (Table 5) differ by 4−32 kcal/mol.[3,95]

Contrary to the BDH data, measured vibrational frequencies are in excellent agreement with the CX^+ stretching frequency obtained in this work. Wu and co-workers[14] studied the photolytic decomposition of CH_3F in neon at 3 K and observed various species including cation **16**. They measured vibrational frequencies of 1759.9 and 1762.9 cm^{-1} for CF^+, which are close to the anharmonically corrected value of 1763 cm^{-1} obtained in this work. Neufeld and Wolfire[18] investigated reactions involving HF, CF^+, and HCl in diffuse and dense interstellar molecular clouds. The ion CF^+ is observed in the Orion Bar region of the Orion Nebula whereas CCl^+ could not be detected.[18]

Influence of Halogen on the Stability of Carbenium Ions. An increase of the CX double bond character in halogen-substituted carbenium ions leads to increased stability. This can be quantified by determining the energy of the formal reactions

$$^+CH_3 + H_3CX \rightarrow {}^+CH_2X + CH_4$$

$$^+CH_2F + H_3CX \rightarrow {}^+CH_2X + H_3CF$$
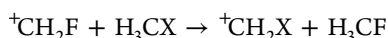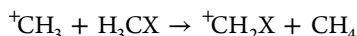
In the first case, the exothermicity of the reaction increases from 29.8 (X = F) to 39.8 (Cl) and 41.4 kcal/mol (Br) according to G3 calculations and to 40.4 kcal/mol (I) according to 2c-NESC/CCSD(T) calculations reflecting the increased stabilization of the carbenium ion by the higher halogens. This is in line with the RBSO values insofar as they indicate larger double bond character as a result of the increasingly larger polarizability and π-donor ability of Cl, Br, or I, Cl, Br, and I stabilize the carbenium ion by 10.0, 11.6, and 10.6 kcal/mol more than F does as is defined by the exothermicity of the second reaction above. Because the I value was obtained by 2c-NESC/CCSD(T) and does not contain the complete basis set effect, it is underestimated and should be closer to 12 kcal/mol. This would be in better agreement with the RBSO values of **1** discussed in the previous subsection.

If the carbenium carbon has substituents, which by either π-conjugation or hyperconjugation can donate electron density, the π-character of the CX^+ bond can be affected. This is the situation of cations **2–5** where methyl or phenyl groups electronically change the situation of the CX^+ bond, which is reflected by its lengthening (F: from 1.226 to 1.297 Å), a decrease in the BDE values (F: from 155.3 to 130.3 kcal/mol), local stretching frequencies (F: from 1618 to 1297 cm^{-1}), local stretching force constants (F: from 11.34 to 7.29 mdyn/Å), and the RBSO values n^{C-E} (F: from 1.713 to 1.263).

Obviously, the phenyl group has a stronger impact on the CX^+ bond than the methyl group where a remote p-phenyl substituent, as in **5**, leads to an additional weakening of the CX bond. When the RBSO values of the F-substituted carbenium ions are plotted against those of the corresponding Cl-, Br-, and I-substituted ions, a stepwise decreased sensitivity against conjugative and hyperconjugative effects is observed for the latter (Table 4). This suggests that the limited π-donor ability of F makes the CF bond sensitive to environmental effects whereas the increased polarizability and donor ability of Br or I are less affected by the presence of other π-donors.

Carbenium ions with π-acceptor substituents such as the carbonyl group(s) in **6** or **7** have a somewhat higher CX double bond character where these effects are larger for the heavier halogens than for F. The CF bond registers any change in the $2p\pi(C)$ orbital energy or overlap with the orbitals of the other bonding partners, which is reflected by the RBSO values and other bond properties of the CX^+ bonds in ions **6–12**. In general, any electron-donor substituent has a stronger impact on the CX^+ bond than an electron-acceptor substituent.

Substitution by another halogen atom as in **13**, **14**, or **15** decreases the RBSO value due to competitive π-donation from two rather than one halogen atom. Again, this confirms that the π-character of the CX^+ bond in carbenium ions is a sensitive detector of hyperconjugative and conjugative effects as well as σ-electron withdrawal and orbital contraction where the sensitivity is in most cases larger for the CF^+ than for the CCl^+, CBr^+, or CI^+ bonds.

CX^+ Bonding in Halonium Ions. The study of halonium ions reaches back to the 1930s when Roberts and Kimball[19] explained the stereospecifity of the bromine addition to alkenes by the intermediacy of bromonium ions. A systematic investigation of halonium ions was carried out by Olah and co-workers[20,21] who generated bridged halonium ions in superacid solutions and characterized them by spectroscopic methods. A large number of experimental and computational investigations on halonium ions has been published, which provided a detailed insight into their properties.[20−27] Dialkylhalonium ions with X = Cl, Br, I turned out to be efficient alkylation agents in synthesis.[29,30] They also react with a base via proton transfer thus forming dialkylhalonium ylides, which produce carbenes and alkenes. One has speculated that dialkylhalonium ylids are key intermediates in the catalyzed formation of alkenes from halomethanes.[35]

The ongoing interest into halonium ion chemistry is reflected by a number of investigations. Ohta and co-workers[36] demonstrated the decisive role of intermediate bridged halonium ions when SO_2 is added to halocarbenium ions where the halonium ion intermediate decides on the stereo-chemistry and mechanism of the reaction. Stoyanov and co-workers[37] determined the X-ray structures of the dimethyl and diethyl chloronium ion as carborane salts. They obtained CCl bond lengths of 1.810 and 1.840 Å and were able to measure some typical vibrational frequencies: The asymmetric and symmetric CClC stretching frequencies of 636 and 596 cm^{-1}, respectively, are in line with our calculated values of 650 and 603 cm^{-1}. Dimethylhalonium ions and their ylides were investigated by Jubert and co-workers,[38] who concluded that the CX bonds in halonium ions are of weak covalent character.

The halonium ions **20–24** can be described formally as charged disubstituted halogens (Figure 1). This implies that an X^+ ion is present, which, in view of the large electronegativity of the halogens is not likely. Instead, the divalent halogen withdraws negative charge from the bonding partners to reduce its positive charge. A somewhat more realistic description of the bonding in halonium ions assumes 4-electron−3-center (4e−3c) bonding where two of the four electrons are taken from the X^+ bonding partners and two from X^+. Because two electrons occupy a 3c-bonding orbital and two remain in a nonbonding orbital, electron-deficient CX^+ bonds are established.

All studies on halonium ions[15,35,37,96] describe their CX bonds as relatively weak and the stability of the ions as low. This is confirmed by the CX stretching force constants k^a and RBSO values n^{C-E} obtained in this work. The RBSO values of the fluoronium ions suggest the existence of fractional CF bonds ($n < 1$). Bridged halonium ions have stronger bonds ($0.52 < n^{C-E} < 0.77$) for the lower halogens X = F, Cl, Br than their acyclic analogues ($0.32 < n^{C-E} < 0.74$). However, for X = I the situation is reversed as **21** has a stronger CI bond (0.84) than the cyclic **20** (0.76, Table 4). The calculated G3 energy differences predict the bridged halonium ion **20** to be 1.8

Table 6. Comparison of Bond Lengths r, BDE Values, Local Stretching Force Constants k^a, and RBSO Values n for Bonds CX and CE in the Form of a Linear Regression Analysis[a]

	CF			CCl		CBr	CO	CS			CSe	
	CCl	CBr	CI	CBr	CI	CI	CS	CSe	CTe	CSe	CTe	CTe
r	0.891	0.848	0.746	0.994	0.953	0.978	0.961	0.951	0.903	0.997	0.978	0.988
	0.030	0.034	0.040	0.006	0.017	0.012	0.016	0.018	0.023	0.004	0.011	0.008
BDE	0.905	0.697	0.318	0.902	0.604	0.850	0.984	0.979	0.938	0.996	0.974	0.850
	8.230	11.400	15.500	6.470	11.800	7.270	3.300	2.350	2.830	1.060	1.840	4.240
k^a	0.928	0.914	0.820	0.997	0.954	0.963	0.981	0.959	0.898	0.995	0.962	0.983
	0.433	0.354	0.372	0.067	0.189	0.168	0.239	0.261	0.284	0.922	0.172	0.114
n	0.931	0.914	0.815	0.997	0.950	0.961	0.982	0.962	0.907	0.995	0.965	0.985
	0.061	0.053	0.060	0.010	0.031	0.028	0.031	0.035	0.041	0.013	0.025	0.017

[a]The parameter of the bond given in the first row is compared with the same parameter of the bond given in the second row in the form of a linear regression analysis. For each analysis, the correlation coefficient R^2 (first entry) and the standard deviation σ (second entry) is given. Bond lengths r in Å, BDE values in kcal/mol, local stretching force constants k^a in mdyn/Å, and RBSO values n.

(X = F), 18.4 (Cl), 21.2 (Br), and 24.7 kcal/mol (I) more stable than its isomer **21**. We note in this connection that **20** can rearrange to the isomeric **2**, which for X = F is 27.1 kcal/mol ($\Delta H(298)$: 28.5 kcal/mol; G3 calculations) more stable.

The small stabilization energy of the fluoronium ion **20** can be rationalized by considering that a relatively strong FH$^+$ bond is formed in **21**, which compensates for the loss of one fractional CF bond. For X = I, the opposite is true because the HI$^+$ bond is weaker than the fractional IC bond and accordingly the bridged form is more stable than one would expect on the basis of the CI bond strength in **21** as compared to that in **20**.

The calculated RBSO values $n^{\text{C}-\text{E}}$ of the halonium ions with Cl, Br, or I are close to 0.8 or 0.9 and reveal that with increasing atomic number of X the halonium ions gain almost the strength of a C—E single bond, again revealing that the less electronegative halogen atoms with their increased π-donor ability are better suited for forming halonium ions. A further increase of the strength of the CX halonium bond is gained as a result of hyperconjugative stabilization caused by alkyl groups as in **22** or **24**. The dimethyl iodonium ion **24**, has the highest RBSO value $n^{\text{C}-\text{E}} = 0.89$ (Table 4). The corresponding BDE value is 81 kcal/mol and the local CI stretching parameters are $\omega^a = 545$ cm^{-1} and $k^a = 1.919$ mdyn/Å (Table 3). Clearly, electron-donating groups can stabilize CX bonding in halonium ions.

The situation is different for the dications **23** where the positively charged allyl part, i.e., an electron-withdrawing group, is bonded to the $^+$XH group (Figure 2). Strong charge repulsion should hinder the formation of a covalent CX bond. However, a 90° rotation of the $^+$XH group leads to an interaction of the empty pπ orbital of $^+$XH with the σ-CC bonds via hyperconjugation. A surprisingly strong CX bond is established in this way: F, $n^{\text{C}-\text{E}} = 0.51$; Cl, 0.83; Br, 0.88; I, 0.94 (Table 4). The calculated BDE values suggest a similar increase in the bond strength: F, 33.7; Cl, 63.1; Br, 72.5; I, 81.1 kcal/mol (Table 2).

Changes in Bonding from Period to Period. In chemistry, there is a tendency of expecting similar trends in bonding for the higher homologues of a given group. Although this may be confirmed in some cases, we cannot identify such a similarity for the current investigation of CX and CE bonds. To clarify this point, we have used the following working hypothesis. The smallest changes in bonding should occur upon moving from a given period in the periodic table to the next higher period. However, large changes can be expected when, e.g., CF and CI bonding are compared. To justify this assumption, we have used linear regression analysis to correlate a given CX or CE bond parameter (X, E belonging to the same period) with the corresponding parameters of CX or CE bonds from different periods. The results of this analysis are summarized in Table 6 in the form of the resulting correlation coefficients R^2 and standard deviations σ.

The results of the analysis can be summarized in the following way.

(1) The best basis for the comparison is provided by the stretching force constants k^a and the RBSO values n where the latter are slightly better suited than the former, reflected by the larger correlation coefficients. This confirms that the bond lengths and BDE values are not reliable bond strength descriptors.

(2) Significant correlations are found when comparing CCl bonds with CBr or CS bonds with CSe. This is in line with the fact that for group 8 and 9 atoms the 3d electrons behave as core electrons and do not lead to a change in bonding for Se and Br.

(3) The correlation between CBr and CI or CSe and CTe bonds is no longer significant, as reflected by the smaller correlation coefficients. The decrease in significance is larger for the CX than the CE bonds. Clearly, this can result from the larger impact of scalar relativistic effects, which leads to a change in the bonding mechanism. In this connection, a caveat is needed insofar as part of this change may result from a lower computational accuracy.

(4) Not unexpected is the fact that bonds formed by second period atoms play an exceptional role. For example, the CF and CO bond properties compare less well with those of the CCl and CS bonds as the latter do with regard to the CBr and CSe bonds. This is a direct result of the efficient hybridization mechanism typical of second period atoms, which leads to significantly stronger bonds than found when atoms of higher periods are involved.

(5) In general, it is confirmed that the larger the difference in atomic numbers, the more different is the bonding mechanism. Therefore, CF and CO bonds are increasingly different from those bonds with X and E from the fourth or fifth period.

These observations are valid for the situation that one (X or E) rather than both bonding partners are changed. As noted above, this leads to special situations with regard to bonding overlap, charge transfer, bond polarity, and bond polarizability.

Relevance of Results for Organic Chemistry. The determination of the bond strength order provides a basis to predict the outcome of organic reactions involving carbon–halogen bonds. For example, the formation of halogen-substituted carbenium ions will preferentially lead to α- rather than β-substituted carbenium ions provided both possibilities

are given. The preferred formation of α-halogen-substituted carbenium ions will increase with increasing atomic number of halogen X. This is also of relevance for halogen-substituted Jahn−Teller and pseudo-Jahn−Teller systems such as the cyclopropane radical cation, the cyclopentadienyl cation, or the benzene radical cation.[97] For halogen-substituted systems, the position of the halogen atom determines the barrier of bond pseudorotation, bond pseudo-libration, or bond pseudo-inversion as was shown recently by Zou and Cremer.[97] In the case of perhalogenated cyclopentadienyl cations, the barrier of bond pseudorotation becomes smaller than 0.3 kcal/mol and molecules without a fixed structure are obtained.[98]

HX elimination reactions will increasingly follow an E1 mechanism if X has an increasingly larger atomic number. Elimination will be facilitated if a hyperconjugative donor in the form of a methyl or alkyl group is present, which will effectively reduce the π-bond character of the CX bond of the α-halogeno carbenium ion as shown in this work. The methyl group will act at the same time as a proton donor in the course of the HX elimination.[9,24] Similarly, in substitution reactions, the S_N1 mechanism will be more and more preferred in the series X = F, Cl, Br, I. In view of the weakening of the CX bond in carbenium ions with increasing atomic number of X, α-iodo-substituted carbenium ions are the ideal precursors for the photolytic generation of carbene radical cations.[99−101]

Although some of these predictions may also be derived on the basis of the available experimental data, we emphasize that the present predictions can be always quantified in situations where closely related structures exclude a differentiation on qualitative grounds. With either observed or calculated vibrational frequencies, a quantitative measure of bond strength is readily available via the local mode stretching force constants to predict the most likely mechanism being followed and the most likely structure being formed. This holds also for the halonium ions. The lifetime of a bridged halonium ion, e.g., being formed in a halogen−alkene addition reaction, will increase from X = F to I. Also, by the choice of the halogen, the stability of dialkyl halonium ions can be tailored so that for a given alkylation purpose a more (X = Cl) or less (X = I) reactive alkylation agent can be enforced. The prediction of stability via the RBSO values will also help to synthesize halonium ions for structural and thermodynamical analysis. Although Olah and others have collected a large amount of synthetic and mechanistic insight into halonium chemistry, the work presented provides a generally applicable tool to quantify the strength of any halogen−carbon bond.

Finally, it has to emphasized that the use of bond length and BDE as bond strength descriptors becomes increasingly questionable if bonding to relativistic elements such as Se, Te, Br, or I is considered. Scalar relativistic contractions and spin−orbit coupling lead to changes in bond length or BDE values, which can no longer be foreseen on the basis of the knowledge gathered for bonds between lighter (nonrelativistic) elements.

5. CONCLUSIONS

Vibrational spectroscopy is an excellent tool to provide detailed information about chemical bonding. To obtain this information, one has to extract from the normal vibrational modes the local vibrational modes and their properties. The local stretching force constant is a bond parameter that measures the strength of a bond without implying a change in the electronic structure of the molecule. Once local stretching force constants k^a are obtained, it is straightforward to derive

suitable bond strength descriptors in the form of the RBSO values n^{C-O} or n^{C-E} used in this work. The k^a values of different bond types formed from atoms throughout the periodic table can be converted by a single equation into RBSO values n^{C-O} using only two suitable reference bonds where the CO single and double bond in methanol and formaldehyde have been chosen in this investigation.

From a thermodynamical point of view a single definition of n in the form of n^{C-O} is sufficient to discuss the changes in the CX or CE bond strength in dependence of X and E. However, it is easier for the chemist to consider bonding with regard to a standard C−E single bond in H_3C−SH, H_3C−SeH, or H_3C−TeH. Therefore, we have used for the discussion RBSO values n^{C-E} and even sometimes $n^{C=E}$ when it was appropriate to compare with the standard CE single or double bond. This was done by using the same k^a−n^{C-O} relationship but by scaling RBSO values to n^{C-E} or $n^{C=E}$ values based on the appropriate C−E or C=E reference bonds. Our investigation has led to the following conclusions.

(1) Calculations reveal that anharmonically corrected vibrational frequencies are desirable to directly compare calculated and measured normal or local mode frequencies. However, for an analysis of trends in bonding, reliable harmonic frequencies are sufficient as they lead to the same conclusions.

(2) Although it is common in chemistry to predict trends in bonding by comparing bond lengths and BDE values, both are unreliable bond strength descriptors. The bond length varies with atomic charges, bond polarity, the number of core shells, and scalar relativistic effects, which change the bond length irrespective of possible changes in bond strength. On a more qualitative basis, the Badger relationship is fulfilled for the bonds investigated in this work.

(3) The BDE depends on the stabilization of the dissociation fragments due to electron density relaxation, geometry changes, or changes in scalar relativistic or spin−orbit coupling effects. In addition, any avoided crossing of the dissociation curve leads to a significant change in the BDE value. Accordingly, the BDE does not provide a reliable or useful description of the strength of the CX and CE bonds investigated in this work.

(4) The C^+ atom of a carbenium ion can establish a partial double bond to halogen X, which stabilizes the ion by up to 41 kcal/mol in the case of X = Br or I. The BDE values of CX increase from 114 to 155 (X = F), 86 to 137 (Cl), 73 to 125 (Br), and 58 to 118 kcal/mol (I) when H_3C−X is replaced by H_2CX^+, again suggesting the strongest stabilization by Br and I. This is confirmed by the k^a-based RBSO values n^{C-E}. For X = Br or I the CX double bond is realized as a result of the larger polarizability and π-donor ability of bromine and iodine.

(5) The CX^+ ion is isoelectronic with C≡E; however, it does not possess a triple bond because the halogen is too electronegative to establish two π-bonds with carbon. Despite BDEs of 181 (X = F), 153 (Cl), 140 (Br), and 128 kcal/mol (I), the RBSO values n^{C-E} of 2.05, 1.91, 1.80, and 1.67 suggest decreasing partial π-bond character. Hence, previous speculations that CF^+, CCl^+, or CBr^+ have a triple bond[12] cannot be confirmed.

(6) The (partial) CX π-bond in halogen-substituted carbenium ions is a sensitive antenna for conjugative and hyperconjugative interactions between the C^+ atom and carbenium ion substituents. Conjugative or hyperconjugative π-donor substituents reduce the CX double bond character, which is directly registered by the local CX stretching force constant and the associated RBSO value. Electron-withdrawing substituents have weaker effects, but they

lead to an increase of the double bond character. The sensitivity of the CF$^+$ bond to other electronic effects in substituted carbenium ions is significantly larger than that of other CX$^+$ bonds. This is a result of the reduced π-donor ability of the F atom as compared to that of Cl, Br, or I.

(7) Halonium ions with divalent F possess fractional covalent bonds, which can be characterized as electron-deficient 4e–3c bonds due to the reluctance of the electronegative F atom to donate an electron lone pair for establishing fully developed C—X single bonds. However, this tendency changes for Br and I, which establish bonds as strong as a typical CX single bond, especially when electropositive groups with donor ability such as alkyl are bonded to X.

(8) According to the calculated RBSO values CX bonding in bridged halonium ions becomes increasingly stronger in the series X = F, Cl, Br, I . Bridged halonium ions are 1.8 (X = F), 18.4 (Cl), 21.2 (Br), and 24.7 kcal/mol (I) more stable than their acyclic counterparts according to G3 calculations. Dissociation into ethene and X$^+$ requires 85, 82, 76, and 72 kcal/mol, respectively. A halonium dication in the form of **23** is surprisingly stable due to a rotation of the XH$^+$ group into a position perpendicular to the allyl cation plane and hyperconjugative stabilization of the CX$^+$ bond. The corresponding BDE values increase from 34 (X = F) to 93 kcal/mol (I).

(9) Carbon—chalcogen double bonds show a similar dependence on substituent effects as the corresponding (partial) CX$^+$ double bonds. However, the variation in the bond strength is much smaller due to a π-bond, which is better shared between carbon and chalcogen. C═E double bonding in the formaldehyde analogues with E = S, Se, or Te decreases rapidly from $n^{C—E}$ = 2.00 (O) to 1.82 (S), 1.74 (Se), and 1.64 (Te), suggesting a reduction of π-bonding in telluroformaldehyde to two-thirds of its strength in the parent molecule. A C≡E triple bond in diatomic CE is only partially or not at all realized according to RBSO values of 2.61 (E = O), 2.18 (S), 2.02 (Se), and 1.85 (Te), which suggest for the higher homologues double bonds.

(10) A systematic study of the CX and CE bond parameters for the four X/E combinations F/O, Cl/S, Br/Se, and I/Te investigated in this work reveals that CF and CO bonds are stabilized by a significantly different bonding mechanism (characterized by perfect bond orbital overlap and larger bond polarities) than CCl/CS or CBr/CSe bonds, which are closely related. CI and CTe bonds, in turn, differ from their lower homologues due to relativistic effects.

This work has demonstrated that multiple bonding is easily and reliably described with the help of vibrational spectroscopy. The RBSO values can be the basis for useful predictions concerning synthesis, chemical reactivity, or materials design. For example, on the basis of this work, the synthesis of relative stable iodonium ions seems to be possible, which could extend their use as attractive alkylation agents.

■ ASSOCIATED CONTENT

Ⓢ Supporting Information

Tables with anharmonically corrected local mode properties; diagrams of RBSOs as a function of the local mode force constants, local stretching force constants compared with bond lengths, and BDEs compared with RBSO values; and tables with Cartesian coordinates and frequencies of all molecules investigated. This material is available free of charge via the Internet at http://pubs.acs.org.

■ AUTHOR INFORMATION

Corresponding Author

*E. Kraka: e-mail, ekraka@gmail.com.

Notes

The authors declare no competing financial interest.

■ ACKNOWLEDGMENTS

■ REFERENCES

(1) Patai, S. *The Chemistry of The Carbon-Halogen Bond, Parts 1 and 2*; Wiley: New York, 1973.

(2) Patai, S.; Rappoport, Z. *The Chemistry of Halides, Pseudo-Halides and Azides, Supplement D2, Parts 1 and 2*; Wiley: New York, 1995.

(3) Luo, Y.-R. *Comprehensive Handbook of Chemical Bond Energies*; Taylor and Francis: Boca Raton, FL, 2007.

(4) Porterfield, W. W. *Inorganic Chemistry, A Unified Approach*; Academic Press: San Diego, 1993.

(5) Pauling, L. *The Nature of the Chemical Bond and the Structure of Molecules and Crystals, An Introduction to Modern Structural Chemistry*; Cornell University Press: Ithaca, NY, 1960.

(6) Pérez-Casany, M.; Sánchez-Marín, J.; Nebot-Gil, I. Ab Initio Study on the Mechanism of Tropospheric Reactions of the Nitrate Radical with Haloalkenes: Chloroethene. *J. Am. Chem. Soc.* **2000**, *122*, 11585−11595.

(7) Kiprof, P.; Miller, S. R.; Frank, M. A. Theoretical investigation of sulfur and halogen-substituted carbocations. *J. Mol. Struct. (THEOCHEM)* **2006**, *764*, 61−67.

(8) Raabe, I.; Himmel, D.; Krossing, I. Computational Study of the Enthalpies of Formation, $\Delta_f H°$, and Mean Bond Enthalpies, mBEs, of $H_{4−n}EX_n^{0/−}$ and $H_{3−n}EX_n^{+/0}$ (E = C, B; X = F–I). *J. Phys. Chem. A* **2007**, *111*, 13209−13217.

(9) Oomens, J.; Kraka, E.; Nguyen, M. K.; Morton, T. H. Structure, Vibrational Spectra, and Unimolecular Dissociation of Gaseous 1-Fluoro-1-phenethyl Cations. *J. Phys. Chem. A* **2008**, *112*, 10774−10783.

(10) Kraka, E.; Cremer, D. Characterization of CF bonds with multiple-bond character: bond lengths, stretching force constants, and bond dissociation energies. *ChemPhysChem* **2009**, *10*, 686−698.

(11) Oomens, J.; Morton, T. H. Fluoronium metathesis and rearrangements of fluorine-stabilized carbocations. *Int. J. Mass Spectrom.* **2011**, *308*, 232−238.

(12) Pyykkö, P.; Riedel, S.; Patzschke, M. Triple-Bond Covalent Radii. *Chem.—Eur. J.* **2005**, *11*, 3511−3520.

(13) Pein, B.; Seong, N.-H.; Dlott, D. Vibrational Energy Relaxation of Liquid Aryl-Halides X-C$_6$H$_5$ (X = F, Cl, Br, I). *J. Phys. Chem. A* **2010**, *114*, 10500−10507.

(14) Wu, Y.-J.; Chen, H.-F.; Chou, S.-L.; Lin, M.-Y.; Cheng, B.-M. Vacuum-ultraviolet photolysis of H$_3$CF in solid neon: Infrared spectra of HCF and CF$^+$. *Chem. Phys. Lett.* **2010**, *497*, 12−17.

(15) Zunino, F.; Liu, F.; Berrier, C.; Martin-Mingot, A.; Thibaudeau, S.; Jouannetaud, M.-P.; Jacquesy, J.-C.; Bachmann, C. Gem-difluorination in superacid: The dramatic role of halonium ions. *J. Fluorine Chem.* **2008**, *129*, 775−780.

(16) Han, I. S.; Kim, C. K.; Sohn, C. K.; Ma, E. K.; Lee, H. W.; Kim, C. K. Comparative Studies on the Reactions of Acetyl and Thioacetyl Halides with NH$_3$ in the Gas Phase and in Aqueous Solution: A Theoretical Study. *J. Phys. Chem. A* **2011**, *115*, 1364−1370.

(17) Pan, Y.; Pan, Y.; Tang, Y.; Tang, Y.; Wang, R.; Wang, R. DFT and ab initio theoretical study for the CF$_3$S + CO reaction. *J. Fluorine Chem.* **2011**, *132*, 15−18.

(18) Neufeld, D. A.; Wolfire, M. G. The Chemistry of Interstellar Molecules Containing the Halogen Elements. *Astrophys. J.* **2009**, *706*, 1594−1604.

(19) Roberts, I.; Kimball, G. E. The Halogenation of Ethylenes. *J. Am. Chem. Soc.* **1937**, *59*, 947−948.

(20) Olah, G. A. *Halonium Ions*; Wiley: New York, 1975.

(21) Olah, G. A.; Laali, K. K.; Wang, Q.; Prakash, G. K. S. *Onium Ions*; Wiley: New York, 1998.

(22) Hamilton, T. P.; Schaefer, H. F. Structure and energetics of $C_2H_4Br^+$: ethylenebromonium ion vs. bromoethyl cations. *J. Am. Chem. Soc.* **1990**, *112*, 8260−8265.

(23) Reynolds, C. H. Structure and relative stability of halogenated carbocations: the $C_2H_4X^+$ and $C_2H_4X^+$ (X = fluoro, chloro, bromo) cations. *J. Am. Chem. Soc.* **1992**, *114*, 8676−8682.

(24) Nguyen, V.; Cheng, X.; Morton, T. Three-membered Cyclic Fluoronium Ions in Gaseous Ion-Neutral Complexes. *J. Am. Chem. Soc.* **1992**, *114*, 7127−7132.

(25) Rodriguez, C. F.; Bohme, D. K.; Hopkinson, A. C. Isomers of $C_2H_4Cl^+$: structures, frequencies, and energetics. *J. Am. Chem. Soc.* **1993**, *115*, 3263−3269.

(26) Damrauer, R.; Leavell, M. D.; Hadad, C. M. Computational Studies of Halonium Ions of Cyclohexene and Cyclopentene. *J. Org. Chem.* **1998**, *63*, 9476−9485.

(27) Olah, G. A.; Rasul, G.; Hachoumy, M.; Burrichter, A.; Prakash, G. K. S. Diprotonated Hydrogen Halides (H_3X^{2+}) and Gitonic Protio Methyl- and Dimethylhalonium Dications (CH_3HX^{2+}) and $(CH_3)_2XH^{2+}$): Theoretical and Hydrogen-Deuterium Exchange Studies. *J. Am. Chem. Soc.* **2000**, *122*, 2737−2741.

(28) Olah, G.; Prakash, G. S.; Rasul, G. Study of the Fluoro- and Chlorodimethylbutyl Cations. *Proc. Natl. Acad. Sci. U. S. A.* **2013**, *110*, 8427−8430.

(29) Olah, G. A.; DeMember, J. R. Friedel-Crafts Chemistry. VI. Alkylation of Heteroorganic Compounds with Dialkylhalonium Fluoroantimonates. A New General Preparation of Onium Ion Salts. *J. Am. Chem. Soc.* **1970**, *92*, 2562−2564.

(30) Olah, G. A.; Mo, Y. K.; Onium Ions, I. X. Intermolecular Exchange Reactions of Dialkylhalonium Fluoroantimonates with Alkyl Halides and Alkylcarbenium Ions. *J. Am. Chem. Soc.* **1974**, *96*, 3560−3564.

(31) Mendoza, A.; Fananas, F. J.; Rodriguez, F. Asymmetric Halocyclizations of Unsaturated Compounds: An Overview and Recent Developments. *Curr. Org. Synth.* **2013**, *10*, 384−393.

(32) Otha, B. The structure of Halonium Ions in Superacidic Solutions. *Pure Appl. Chem.* **2013**, *85*, 1959−1965.

(33) Denmark, S.; Kuester, W.; Burk, M. Catalytic, Asymmetric Halofunctionalization of Alkenes - A Critical Perspective. *Angew. Chem., Int. Ed.* **2012**, *51*, 10938−10953.

(34) Satoshi, M. Utilization of N-X Bonds in the Synthesis of N-Heterocycles. *Acc. Chem. Res.* **2009**, *42*, 1172−1182.

(35) Noronha, L.; Judson, T.; Dias, J.; Santos, L.; Eberlin, M.; Mota, C. Intrinsic Acidity of Dimethylhalonium Ions: Evidence for Hyperconjugation in Dimethylhalonium Ylides in the Gas Phase. *J. Org. Chem.* **2006**, *71*, 2625−2629.

(36) Ohta, B. K.; Scupp, T. M.; Dudley, T. J. Theoretical Evidence for the Nucleophilic Addition of Sulfur Dioxide to 1,2-Bridged Chloronium and Bromonium Ions. *J. Org. Chem.* **2008**, *73*, 7052−7059.

(37) Stoyanov, E.; Stoyanova, I.; Tham, F.; Reed, C. Dialkyl Chloronium Ions. *J. Am. Chem. Soc.* **2010**, *132*, 4062−4063.

(38) Jubert, A.; Okulik, N.; Michelini, M.; Mota, C. Topological Insights into the Nature of the Halogen-Carbon Bonds in Dimethylhalonium Ylides and Their Cations. *J. Phys. Chem. A* **2008**, *112*, 11468−11480.

(39) Struble, M.; Scerba, M.; Siegler, M.; Lectka, T. Evidence for a Symmetrical Fluoronium Ion in Solution. *Science* **2013**, *340*, 57−60.

(40) Cremer, D.; Wu, A.; Kraka, E. Some Thoughts About Bond Energies, Bond Lengths, and Force Constants. *J. Mol. Model.* **2000**, *6*, 396−412.

(41) Kalescky, R.; Kraka, E.; Cremer, D. Identification of the Strongest Bonds in Chemistry. *J. Phys. Chem. A* **2013**, *117*, 8981−8995.

(42) Decius, J. Compliance Matrix and Molecular Vibrations. *J. Chem. Phys.* **1963**, *38*, 241−248.

(43) McKean, D. C. Individual CH Bond Strengths in Simple Organic Compounds: Effects of Conformation and Substitution. *Chem. Soc. Rev.* **1978**, *7*, 399−422.

(44) Duncan, J. L.; Harvie, J. L.; McKean, D. C.; Cradock, C. The Ground-State Structures of Disilane, Methyl Silane and the Silyl Halides, and An SiH Bond Length Correlation with Stretching Frequency. *J. Mol. Struct.* **1986**, *145*, 225−242.

(45) Murphy, W. F.; Zerbetto, F.; Duncan, J. L.; McKean, D. C. Vibrational-Spectrum and Harmonic Force-Field of Trimethylamine. *J. Phys. Chem.* **1993**, *97*, 581−595.

(46) Henry, B. R. The Local Mode Model and Overtone Spectra: A Probe of Molecular Structure and Conformation. *Acc. Chem. Res.* **1987**, *20*, 429−435.

(47) Brandhorst, K.; Grunenberg, J. How Strong Is It? The Interpretation of Force and Compliance Constants as Bond Strength Descriptors. *Chem. Soc. Rev.* **2008**, *37*, 1558−1567.

(48) Vijay Madhav, M.; Manogaran, S. A Relook at the Compliance Constants in Redundant Internal Coordinates and Some New Insights. *J. Chem. Phys.* **2009**, *131*, 174112−174112-6.

(49) Grunenberg, J.; Goldberg, N. How Strong Is the Gallium≡ Gallium Triple Bond? Theoretical Compliance Matrices as a Probe for Intrinsic Bond Strengths. *J. Am. Chem. Soc.* **2000**, *122*, 6045−6047.

(50) Brandhorst, K.; Grunenberg, J. Efficient Computation of Compliance Matrices in Redundant Internal Coordinates From Cartesian Hessians for Nonstationary Points. *J. Chem. Phys.* **2010**, *132*, 184101−184101-7.

(51) Espinosa, A.; Streubel, R. Computational Studies on Azaphosphiridines, or How to Effect Ring-Opening Processes through Selective Bond Activation. *Chem. - Eur. J.* **2011**, *17*, 3166−3178.

(52) Kraka, E.; Larsson, J. A.; Cremer, D. In *Computational Spectroscopy: Methods, Experiments and Applications*; Grunenberg, J., Ed.; Wiley: New York, 2010; p 105.

(53) Konkoli, Z.; Cremer, D. A New Way of Analyzing Vibrational Spectra. I. Derivation of Adiabatic Internal Modes. *Int. J. Quantum Chem.* **1998**, *67*, 1−9.

(54) Cremer, D.; Larsson, J. A.; Kraka, E. In *Theoretical and Computational Chemistry, Vol. 5, Theoretical Organic Chemistry*; Parkanyi, C., Ed.; Elsevier: Amsterdam, 1998; p 259.

(55) Kalescky, R.; Zou, W.; Kraka, E.; Cremer, D. Local vibrational modes of the water dimer - Comparison of theory and experiment. *Chem. Phys. Lett.* **2012**, *554*, 243−247.

(56) Kalescky, R.; Kraka, E.; Cremer, D. Local vibrational modes of the formic acid dimer - the strength of the double hydrogen bond. *Mol. Phys.* **2013**, *111*, 1497−1510.

(57) Konkoli, Z.; Cremer, D. A New Way of Analyzing Vibrational Spectra. III. Characterization of Normal Vibrational Modes in Terms of Internal Vibrational Modes. *Int. J. Quantum Chem.* **1998**, *67*, 29−40.

(58) Zou, W.; Kalescky, R.; Kraka, E.; Cremer, D. Relating normal vibrational modes to local vibrational modes with the help of an adiabatic connection scheme. *J. Chem. Phys.* **2012**, *137*, 084114−084114−11.

(59) Zou, W.; Kalescky, R.; Kraka, E.; Cremer, D. Relating normal vibrational modes to local vibrational modes benzene and naphthalene. *J. Mol. Model.* **2012**, 1−13.

(60) Wilson, E. B.; Decius, J. C.; Cross, P. C. *Molecular Vibrations. The Theory of Infrared and Raman Vibrational Spectra*; McGraw-Hill: New York, 1955.

(61) Hayward, R. J.; Henry, B. R. A General Local-Mode Theory for High Energy Polyatomic Overtone Spectra and Application to Dichloromethane. *J. Mol. Spectrosc.* **1975**, *57*, 221−235.

(62) Kjaergaard, H. G.; Yu, H.; Schattka, B. J.; Henry, B. R.; Tarr, A. W. Intensities in local mode overtone spectra: Propane. *J. Chem. Phys.* **1990**, *93*, 6239−6248.

(63) Kjaergaard, H. G.; Turnbull, D. M.; Henry, B. R. Intensities of CH- and CD-stretching overtones in 1,3-butadiene and 1,3-butadiene-d_6. *J. Chem. Phys.* **1993**, *99*, 9438−9452.

(64) Rong, Z.; Henry, B. R.; Robinson, T. W.; Kjaergaard, H. G. Absolute Intensities of CH Stretching Overtones in Alkenes. *J. Phys. Chem. A* **2005**, *109*, 1033−1041.

(65) Jacob, C. R.; Luber, S.; Reiher, M. Understanding the signatures of secondary-structure elements in proteins via Raman optical activity spectroscopy. *Chem.—Eur. J.* **2009**, *15*, 13491−13508.

(66) Jacob, C. R.; Reiher, M. Localizing Normal Modes in Large Molecules. *J. Chem. Phys.* **2009**, *130*, 084106−084106-15.

(67) Liegeois, V.; Jacob, C. R.; Champagne, B.; Reiher, M. Analysis of Vibrational Raman Optical Activity Signatures of the (TG)N and (GG)N Conformations of Isotactic Polypropylene Chains in Terms of Localized Modes. *J. Phys. Chem. A* **2010**, *114*, 7198−7212.

(68) Sokolov, V. I.; Grudzev, N. B.; Farina, I. A. Local Vibrational Mode in Zinc Telluride Associated with a Charged Nickel Impurity. *Phys. Solid State* **2003**, *45*, 1638−1643.

(69) Sangster, M. J. L.; Harding, J. H. Calculation of local and gab mode frequencies from impurities in alkali halide crystals. *J. Phys. C, Solid State Phys* **1986**, *19*, 6153−6158.

(70) Badger, R. M. A Relation Between Internuclear Distances and Bond Force Constants. *J. Chem. Phys.* **1934**, *2*, 128−131.

(71) Truhlar, D. G. The M06 suite of density functionals for main group thermochemistry, thermochemical kinetics, noncovalent interactions, excited states, and transition elements: two new functionals and systematic testing of four M06-class functionals and 12 other functionals. *Theor. Chem. Acc.* **2008**, *120*, 215−241.

(72) Dunning, T. H. Gaussian Basis Sets for Use in Correlated Molecular Calculations. I. the Atoms Boron Through Neon and Hydrogen. *J. Chem. Phys.* **1989**, *90*, 1007−1023.

(73) Kendall, R.; Dunning, T., Jr.; Harrison, R. J. Electron affinities of the first-row atoms revisited. Systematic basis sets and wave functions. *J. Chem. Phys.* **1992**, *96*, 6796−6806.

(74) Peterson, K. A.; Figgen, D.; Goll, E.; Stoll, H.; Dolg, M. Systematically convergent basis sets with relativistic pseudopotentials. II. Small-core pseudopotentials and correlation consistent basis sets for the post-d group 16−18 elements. *J. Chem. Phys.* **2003**, *119*, 11113−11123.

(75) Kozuch, S.; Martin, J. M. L. Halogen Bonds: Benchmarks and Theoretical Analysis. *J. Chem. Theory Comput.* **2013**, *9*, 1918−1931.

(76) Borosky, G. L.; Laali, K. K. A computational study (DFT, MP2, and GIAO-DFT) of substituent effects on protonation regioselectivity in β,β-disubstituted vinyldiazonium cations: formation of highly delocalized carbenium/diazonium dications. *J. Phys. Org. Chem.* **2010**, *23*, 115−125.

(77) Keal, T. W.; Tozer, D. J. Selenium chemistry with DFT: molecular structures and Se-77 NMR shielding constants. *Mol. Phys.* **2005**, *103*, 1007−1011.

(78) Barone, V. Anharmonic Vibrational Properties by a Fully Automated Second-Order Perturbative Approach. *J. Chem. Phys.* **2005**, *122*, 014108−014108-10.

(79) Curtiss, L.; Raghavachari, K.; Redfern, P.; Rassolov, V.; Pople, J. Gaussian-3 (G3) theory for molecules containing first and second-row atoms. *J. Chem. Phys.* **1998**, *109*, 7764−7776.

(80) Raghavachari, K.; Trucks, G. W.; Pople, J. A.; Head-Gordon, M. A Fifth-Order Perturbation Comparison of Electron Correlation Theories. *Chem. Phys. Lett.* **1989**, *157*, 479−483.

(81) Zou, W.; Filatov, M.; Cremer, D. An improved algorithm for the normalized elimination of the small-component method. *Theor. Chem. Acc.* **2011**, *130*, 633−644.

(82) Zou, W.; Filatov, M.; Cremer, D. Development and Application of the Analytical Energy Gradient for the Normalized Elimination of the Small Component Method. *J. Chem. Phys.* **2011**, *134*, 244117−244117-11.

(83) Zou, W.; Filatov, M.; Cremer, D. Development, Implementation, and Application of an Analytic Second Derivative Formalism for the Normalized Elimination of the Small Component Method. *J. Chem. Theory Comput.* **2012**, *8*, 2617−2629.

(84) Zou, W.; Filatov, M.; Cremer, D. Analytic calculation of second-order electric response properties with the normalized elimination of the small component (NESC) method. *J. Chem. Phys.* **2012**, *137*, 084108−084108-9.

(85) Filatov, M.; Zou, W.; Cremer, D. Spin-orbit coupling calculations with the two-component Normalized Elimination of the Small Component method. *J. Chem. Phys.* **2013**, *139*, 014106−014106-8.

(86) Nakajima, T.; Hirao, K. The higher-order Douglas−Kroll transformation. *J. Chem. Phys.* **2000**, *113*, 7786−7789.

(87) Koga, T.; Tatewaki, H.; Shimazaki, T. Chemically reliable uncontracted Gaussian-type basis sets for atoms H to Lr. *Chem. Phys. Lett.* **2000**, *328*, 473−482.

(88) Sekiya, M.; Noro, T.; Osanai, Y.; Koga, T. Contracted polarization functions for the atoms Ca, Ga-Kr, Sr, and In-Xe. *Theor. Chim. Acta* **2001**, *106*, 297−300.

(89) Reed, A.; Curtiss, L.; Weinhold, F. Intermolecular Interactions From a Natural Bond Orbital, Donor-Acceptor Viewpoint. *Chem. Rev.* **1988**, *88*, 899−926.

(90) Kraka, E.; Zou, W.; Filatov, M.; Gräfenstein, J.; Gauss, J.; He, Y.; Wu, A.; Konkoli, Z.; He, Z.; Cremer, D. *COLOGNE2013*; Southern Methodist University, Dallas, TX, 2013.

(91) Frisch, M.; et al. *Gaussian 09*, Revision A.1; Gaussian Inc.: Wallingford, CT, 2009.

(92) Cremer, D.; Kraka, E. From Molecular Vibrations to Bonding, Chemical Reactions, and Reaction Mechanism. *Curr. Org. Chem.* **2010**, *14*, 1524−1560.

(93) Schmidt, M. W.; Gordon, M. S. π-Bond Strengths in HP=PH, H2P=P, HP=NH, and HN=NH. *Inorg. Chem.* **1986**, *25*, 248−254.

(94) Schmidt, M. W.; Truong, P. N.; Gordon, M. S. Pi Bonds in Second and Third Period Elements. *J. Am. Chem. Soc.* **1987**, *109*, 5217−5227.

(95) Huber, K. P.; Herzberg, G. *Molecular Spectra and Molecular Structure, IV. Constants of Diatomic Molecules*; Van Nostrand Reinholdl, New York, 1979.

(96) Shellhamer, D. F.; Gleason, D. C.; Rodriguez, S. J.; Heasley, V. L.; Boatz, J. A.; Lehman, J. J. Correlation of calculated halonium ion structures with product distributions from fluorine substituted terminal alkenes. *Tetrahedron* **2006**, *62*, 11608−11617.

(97) Zou, W.; Cremer, D. Description of Bond Pseudorotation, Bond Pseudolibration, and Ring Pseudoinversion Processes caused by the Pseudo-Jahn-Teller Effect: Fluoro-Derivatives of the Cyclopropane Radical Cation. *Aust. J. Chem.* **2014**, in press, DOI: 10.1071/CH13480.

(98) Zou, W.; Filatov, M.; Cremer, D. Bondpseudorotation, Jahn-Teller, and Pseudo-Jahn-Teller Effects in the Cyclopentadienyl Cation and its Pentahalogeno Derivatives. *Int. J. Quantum Chem.* **2012**, *112*, 3174−3187.

(99) Bally, T.; Carra, C.; Matzinger, S.; Truttmann, L.; Gerson, F.; Schmidlin, R.; Platz, M.; Admasu, A. π- and σ-Diazo Radical Cations:? Electronic and Molecular Structure of a Chemical Chameleon. *J. Am. Chem. Soc.* **1999**, *121*, 7011−7019.

(100) Stoub, D.; Goodman, J. Diarylcarbene Cation Radicals: Generation and Chemical Reactivity in Solution. *J. Am. Chem. Soc.* **1997**, *119*, 11110−11111.

(101) Bally, T.; Matzinger, S.; Truttman, L.; Platz, M. S.; Admasu, A.; Gerson, F.; Arnold, A.; Schmidlin, R. Diphenylcarbene Cation: Electronic and Molecular Structure. *J. Am. Chem.* **1993**, *115*, 7007−7008.